Understanding the role of neuronal cell fate determinants in synapse pattern formation in *C. elegans*

by

Mizuki Kurashina

B.Sc., The University of British Columbia, 2017

A THESIS SUBMITTED IN PARTIAL FULFILLMENT OF THE REQUIREMENTS FOR THE DEGREE OF

MASTER OF SCIENCE

in

THE FACULTY OF GRADUATE AND POSTDOCTORAL STUDIES

(Zoology)

THE UNIVERSITY OF BRITISH COLUMBIA

(Vancouver)

October 2020

The following individuals certify that they have read, and recommend to the Faculty of Graduate and Postdoctoral Studies for acceptance, a thesis entitled:

Understanding the role of neuronal cell fate determinants in synapse pattern formation in *C. elegans*

submitted by Mizuki Kurashina in partial fulfillment of the requirements for the degree of Master of Science in Zoology

Examining Committee:

Kota Mizumoto, Zoology
Supervisor

Donald Moerman, Zoology
Supervisory Committee Member

Kenji Sugioka, Zoology
Supervisory Committee Member

Matt Ramer, Zoology
Additional Examiner

Abstract

Animal locomotion and behaviour are ultimately controlled by the precise neuronal circuit formation at the level of synaptic connection. Mutations in the genes that specify individual neuronal cell fate (or cell fate determinants) alter synaptic connections and circuit wiring which results in the malfunction of the nervous system. It is however not fully understood if the defects in these mutants are merely due to a consequence of cell fate transformation, or the cell fate determinants have specific functions in synapse pattern formation. Here we identify a novel role for a homeobox transcription factor UNC-4 and its co-repressor UNC-37/Groucho, in tiled synapse pattern formation of the cholinergic motor neurons (DA8 and DA9) in *Caenorhabditis elegans*. In *unc-4* and *unc-37* mutant animals, we observed large overlap between the synaptic domains of DA8 and DA9. Strikingly, we show using temperature-sensitive mutants and auxin-inducible degron system that *unc-4* is not required during embryonic development when DA neurons cell fate is set but is required post-embryonically. In contrast, *unc-37* is required embryonically and post-embryonically in DA neurons for a tiled synaptic innervation. Our result reveals a novel post-cell fate determination role of homeobox gene in neuronal pattern formation.

Lay Summary

The nervous system is necessary across the animal kingdom for locomotion and behaviour. Cells of the nervous system called neurons communicate with their targets (neurons and muscle cells) using connections known as synapses. Neurons need to connect with their proper targets for the normal functioning nervous system. There are diverse types of neurons with distinct characters. This difference is controlled by a group of molecules called neuronal cell fate determinants, that dictate the neurons molecular features and function. While many neuronal cell fate determinants have been identified, the role of these proteins on the proper connectivity of neurons to their targets is less understood. In this thesis, I use the nematode, *Caenorhabditis elegans*, to understand the role of neuronal cell fate determinants in proper synapse pattern formation. I identified that the neuronal cell fate determinants of the DA neurons are required for the proper synapse pattern formation in two DA neurons: DA8 and DA9. I further found that the role of the neuronal cell fate determinants of the DA neurons in synapse pattern formation is distinct from its known function to control the neurons diversification. This is a new and important distinction that has not been identified before in this field.

Preface

All the works described in this thesis was performed under the supervision of Dr. Kota Mizumoto in the Life Sciences Institute, at the University of British Columbia. Jane Wang, a previous undergraduate researcher and research technician, analyzed the mizIs3 single mutants (*plx-1, unc-4*) and double mutants (*unc-4;plx-1*) used in this study. Arpun Johal, a previous undergraduate researcher, assisted with generating strains. All other experiments have been performed by myself. Dr. Mizumoto and I designed experiments together, and I collected and analyzed all the data

Chapters 3 and 4 have been used for manuscript soon to be submitted.

Table of Contents

List of Tables

List of Figures

List of Abbreviations

ACR	AcetylCholine Receptor
AID	Auxin-Inducible Degron
BFP	Blue Fluorescent Protein
C. elegans	*Caenorhabditis elegans*
CEH	C. Elegans Homeobox
CHE	abnormal CHEmotaxis
COE	Collier/Olf1/EBF (class of homeodomain proteins)
DNA	DeoxyriboNucleic Acid
DA	Dorsal A class
DB	Dorsal B class
DD	Dorsal D class
DNA	DeoxyriboNucleic Acid
GABA	Gamma AminoButyric Acid
GFP	Green Fluorescent Protein
K-NAA	α-Napthaleneacetic Acid (Synthetic Auxin)
L1, L2, L3, L4	Larval stage 1,2,3,4
LIM	Lin11/Isl1/Mec-3 (class of homeodomain proteins)

NGM	Nematode Growth Media
PCR	Polymerase Chain Reaction
Prd	Paired (class of homeodomain proteins)
TTX	abnormal ThemoTaXis
VA	Ventral A class
VAB	Variable ABnormal morphology
VB	Ventral B class
VD	Dorsal D class
unc	UNCoordinated

Acknowledgments

First and foremost, I would like to thank Dr. Kota Mizumoto for his guidance in academia and generally to become a better professional. Although I have stumbled a fair number of times, he has helped me without needing to micromanage and has treated me as a fellow scientist, for this I thank him. I would also like to thank my friends and family for their continuous support in my endeavors. I would also like to thank my peers and lab members (past and present) for their help as I progressed through as a researcher and student. I also thank my committee members for the support and intellect they have provided me in helping me with my research project and in my academic goals.

1. Introduction

1.1 Neuronal cell fate determinants

The nervous system is required for locomotion and behaviour across the animal kingdom. The cells of the nervous system called neurons form connections to create circuits that mediate behaviour. These circuits are formed through the establishment of neurons and their respective neuronal identities. Neuronal identities are distinguished by the gene expression pattern that gives rise to the molecular and functional features in a single neuron or a group of neurons. Neurons that share common molecular and functional features such as neurotransmitter choice, are categorized as a neuronal class. The differences in gene expression and neuronal identities determine the functional traits/properties, such as neurotransmitter choice and morphology in any given neuron. These neuronal identities are regulated by a group of transcription factors called neuronal cell fate determinants. Many of these neuronal cell fate determinants have been identified in specifying and maintaining neuronal identity, in both vertebrate- and invertebrate systems. (Hobert and Kratsios, 2019; Hobert, 2016; Allan and Thor, 2015).

1.1.1 Terminal selectors in *C. elegans*

Several works in *Caenorhabditis elegans* have uncovered a group of neuronal cell fate determinants called terminal selectors, which are master regulator genes required to initiate and maintain terminal identity in postmitotic neurons; and their genetic regulatory networks and respective DNA binding motifs have been elucidated for numerous neuronal types (Uchida et al., 2003; Chang et al., 2003; Etchberger et al., 2007; Flames and Hobert, 2009; Kratsios et al., 2011; Doitsidou et al., 2013; Zhang et al., 2014). Terminal selectors control the morphology and anatomy, and functional and molecular traits of neurons by regulating the expression of common

molecular features (Hobert and Kratsios, 2019; Hobert, 2016; Allan and Thor, 2015). For example, in *C. elegans,* the COE-type transcription factor UNC-3 is expressed in cholinergic motor neurons and are responsible for the expression of a battery of genes required for acetylcholine neurotransmitter synthesis, transport, degradation, and reuptake, and ultimately determine the terminal neuronal fate of cholinergic motor neurons (Kratsios et al., 2011). Similarly, the Pitx2-type homeodomain transcription factor, UNC-30 is expressed in GABAergic motor neurons and is responsible for the expression of the battery of genes required for the use of the neurotransmitter GABA (Jin et al., 1994). The *C. elegans* AIY neuron also utilises terminal selectors, Paired- and LIM-type homeodomain transcription factor CEH-10 and TTX-3, to maintain its terminal neuronal fate (Altun-Gultekin et al., 2001; Wenick and Hobert, 2004). The ASE neuron utilises the zinc-finger transcription factor CHE-1 as its terminal selector to maintain terminal neuronal fate (Uchida et al., 2003).

1.1.2 Neuronal cell fate determinants that function downstream of terminal selectors

Within a neuronal class, groups of neurons with diverse morphologies with different functional and molecular traits are still observed. These different groups of neurons are subcategorized as neuronal subtypes or neuronal subclasses within a neuronal class. Interestingly, subtype-specific traits that distinguish the neuronal subtypes have been found to be regulated by the same terminal selector that control the common molecular features of their neuronal class. The presence of neuronal cell fate determinants that function downstream of terminal selectors delineates individual neuronal subtypes from the larger neuronal class. For example, in the cholinergic motor neuron class defined by UNC-3 in *C. elegans*, there are neuronal subtypes (DA, VA, DB, VB, AS) that are distinguished by neuronal function and morphology. UNC-3 binds to discrete *cis*-regulatory elements of cholinergic class-specific (Ex.

Acetylcholine (ACh) pathway) and subtype-specific effector genes (Ex. A-type and B-type specific genes) (Kerk et al., 2017). For example, the *C. elegans* GABAergic motor neurons, VD and DD, utilise the terminal selector *unc-30* to regulate the expression of genes required for GABA neurotransmitter use (Jin et al., 1994; Eastman et al., 1999; Cinar et al., 2005). The neuronal specification of the VD motor neurons is dependent on the neuronal cell fate determinant *unc-55*, a transcription factor of the nuclear receptor hormone superfamily that functions downstream of *unc-30* (Zhou and Walthall, 1998). *unc-55* is necessary and sufficient to drive VD neuronal specification in both VD and DD motor neurons through the transcriptional repression of DD-specific genes (Ex. *flp-13*) in VD neurons (Zhou and Walthall, 1998; Shan et al., 2005; Thompson-Peer et al., 2012).

1.1.3 Neuronal cell fate determination in vertebrates

Terminal selectors are also present in vertebrate systems. For example, serotonergic neurons that reside in the Raphe nuclei of the brainstem of mice requires the transcription factor PET-1 for its neuronal specification and expression of the serotonergic gene battery (Hendricks et al., 1999) and to control postmitotic development and maturation of these neurons (Wyler et al., 2016). Whereas the cholinergic neurons in the mice central nervous system utilise a conserved LIM homeodomain transcription factor Isl1 (Ericson et al., 1992; Tsuchida et al., 1994; Wang and Liu, 2001; Elshatory et al., 2007) for the expression of cholinergic gene batteries and differentiation of motor neurons in the spinal cord and hindbrain (Pfaff et al., 1996; Liang et al., 2011; Cho et al., 2014).

Neuronal subtype specification in vertebrates utilises similar mechanisms as invertebrate genetic regulatory networks. For example, in the vertebrate photoreceptors, Crx, a paired-homeodomain protein, acts as the terminal selector in rod and cone photoreceptors and is

required for the expression of the common molecular traits of rod and cone photoreceptors (Furukawa et al., 1997; Chen et al., 1997). In rod photoreceptors, two downstream neuronal cell fate determinants, Nrl and Nr2e3, act with Crx to activate rod-specific genes and repress cone-specific genes (Rehemtulla et al., 1996; Chen et al., 1997; Mears et al., 2001; Chen et al., 2005).

1.2 The roles of neuronal cell fate determinants on neuronal wiring

1.2.1 The limitation to studying neuronal cell fate determinants in neuronal patterning

While there have been many studies identifying neuronal cell fate determinants and their transcriptional regulation of the target genes, much less is known about how they affect neuronal wiring specificity. In vertebrate models, mostly in mice, early knockouts of neuronal cell fate determinants have often resulted in neuronal classes that fail to develop or degenerate and thus cannot be further examined (Cheng et al., 2003; Kadkhodaei et al., 2009). For example, the serotonergic neurons in the raphe nuclei in mice utilise the LIM homeodomain transcription factor *Lmx1b* for their specification and terminal differentiation and loss of *Lmx1b* function induces cell death in these serotonergic neurons (Ding et al., 2003).

Studies using *C. elegans* as a model organism to study the nervous system require the use of neuronal cell- and class-specific promoters to drive the expression of fluorescently tagged proteins to visualize neuronal and synaptic morphology. For example, to visualize the neuronal structures in A-type cholinergic motor neurons of *C. elegans*, researchers often use the *unc-4* promoter to drive the expression of synaptic proteins (Winnier et al., 1999; Von Stetina et al., 2007; Mizumoto and Shen, 2013; Chen et al., 2018). However, loss of UNC-3 significantly reduces the strength from the *unc-4* promoter (Kerk et al., 2017). Therefore, studying the role of terminal selectors in neuronal wiring has been difficult.

However, some studies using electron microscopy (EM) reconstruction have been able to shed light on the role of terminal selectors in neuronal wiring and synapse formation in *C. elegans*. Using EM reconstructions to examine the neuronal and synaptic morphology of the GABAergic motor neurons (VD and DD) in *unc-30* mutant animals, Howell et al. showed that the loss of the GABAergic terminal selector *unc-30,* disrupted synaptic patterning in VD and DD motor neurons. A similar approach using EM reconstruction of the well-defined region in the anterior ventral nerve cord in *unc-3* mutant animals has shown defective synaptic connectivity, where the synaptic input onto the AVA interneurons and output from the AVA interneurons were reduced (Pereira et al., 2015). Additionally, the examination of anatomically and spatially unique neurons that are easily distinguishable, such as the SAB motor neurons that reside in the head of *C. elegans*, allowed the discovery of the role of *unc-3* in synaptogenesis (Kratsios et al., 2015). In contrast, studying the role of *unc-3* in the motor neurons that reside in the ventral nerve cord (DA, DB, VA, VB) would be difficult due to the inability to distinguish neuronal structures from the other motor neuron classes.

1.3 A-class and B-class cholinergic motor neuron circuit in *C. elegans*

Among cholinergic motor neurons in *C. elegans*, there are A-class and B-class neurons for their role in backward and forward locomotion, respectively. The dorsal A-type (DA) and ventral A-type (VA) motor neurons are required for the backward locomotion and dorsal B-type (DB) and ventral B-type (VB) motor neurons are required for the forward locomotion. (Chalfie et al., 1985). The cell fates of A-class and B-class of motor neurons are determined by the transcription factor, UNC-4 and its transcriptional co-repressor, UNC-37 (see sections 1.6 and 1.7). Both A- and B-class motor neuron cell bodies reside in the ventral nerve cord (White et al., 1986). While the VA, VB, DA, DB motor neurons use the same terminal selector, UNC-3, they

have distinct axonal morphologies and functions. The VA and VB motor neurons extend their dendrites and axons on the ventral nerve cord and form synapses along the ventral body wall muscle (White et al., 1986). However, the VA and VB motor neurons display opposite axonal trajectories; the VA neuron extends their axon anteriorly, while the VB motor neuron extends their axon posteriorly (Figure 1). The DA and DB motor neuron also reside in the ventral nerve cord and extend their dendrites on the ventral nerve cord and extend their axons first on the ventral side but form a commissure and extend their axons on the dorsal nerve cord where they form synapses (Figure 1). Similar to VA and VB motor neurons, DA and DB motor neurons also

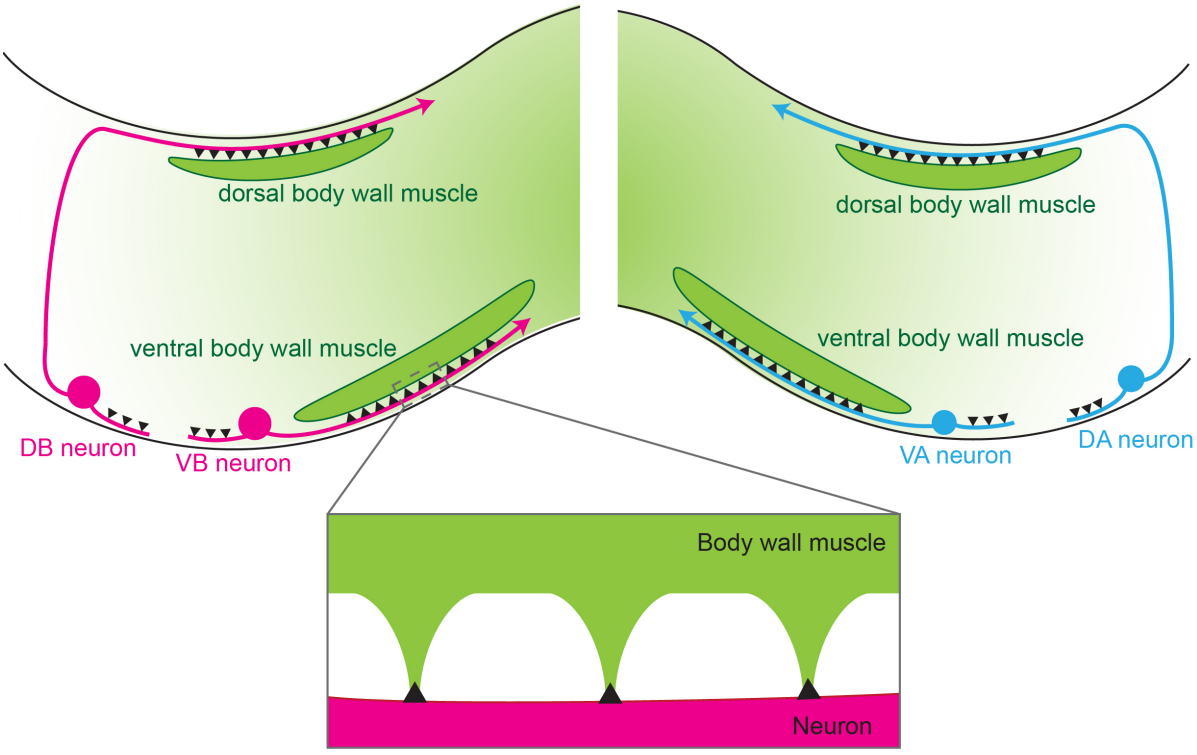

Figure 1. Schematic of A-class and B-class cholinergic motor neurons structure

Schematic of cholinergic motor neurons (DA, VA, DB, VB). Neuronal cell bodies are represented with circles. Axons are represented with lines with an arrow head. Dendrites are represented with lines. Synapses are represented with triangles. The body wall muscles extend muscle arms to neurons for innervation.

display opposite axonal trajectories, where DA motor neurons extend their axons anteriorly and DB motor neurons extend their axons posteriorly. The DA and DB motor neurons are embryonically born and complete their axon guidance before the animal hatches (Sulston, 1983). Interestingly, the DA and DB motor neurons do not share a common lineage and are not sister cells. In comparison, the VA and VB motor neurons are post-embryonically born and share a common lineage (White et al., 1992). The VA and VB motor neurons are considered sister cells.

The A-class cholinergic motor neurons are innervated by the AVA, AVD, and AVE command interneuron which acts as the driver cells that initiate the backward locomotion. AVA and AVD interneurons are innervated by touch receptor cells that respond to anterior touch which include the BDU, SDQR, FLP, ADE, and AQR sensory neurons, creating a reflex circuit for backward locomotion (Chalfie et al., 1985; Li et al., 2011). On the other hand, B-class cholinergic motor neurons are innervated by command interneurons: AVB and PVC. The AVB and PVC interneurons are innervated by touch receptor cells that respond to posterior touch, which include the PVD, PDE, PHA, and PHB sensory neurons (Chalfie et al., 1985; Li et al., 2011)

1.4 Neuronal Patterning in *C. elegans*

1.4.1 Synaptic tiling of *C. elegans*

Previous electron microscopy reconstruction has revealed the tiled synaptic innervation of *C. elegans* motor neurons (White et al., 1976). Each motor neuron forms *en passant* synapses along its axon onto the body wall muscles (White et al., 1976) (Figure 2). The synaptic domain of a neuron does not overlap with those from the neighboring neurons within the same class, thereby creating a tiled presynaptic pattern (Mizumoto and Shen, 2013; Chen et al., 2018)

(Figure 2, 3B and C). It is unclear if each neuronal class has a mechanism to regulate their own synaptic patterning. Our lab has previously shown that the tiled presynaptic pattern between two neighboring DA-class of motor neurons (DA8 and DA9) is mediated by Plexin and its ligand Semaphorin and its downstream signaling pathway (Mizumoto and Shen, 2013; Chen et al., 2018). However, it is also unclear whether Semaphorin-Plexin signaling is the sole coordinator that governs synaptic patterning in DA neurons. As the synaptic tiling is specific to each neuronal class, we speculate that the class-specific synaptic patterning may be under the control of the neuronal cell fate determinants which specify and maintain neuronal class identity.

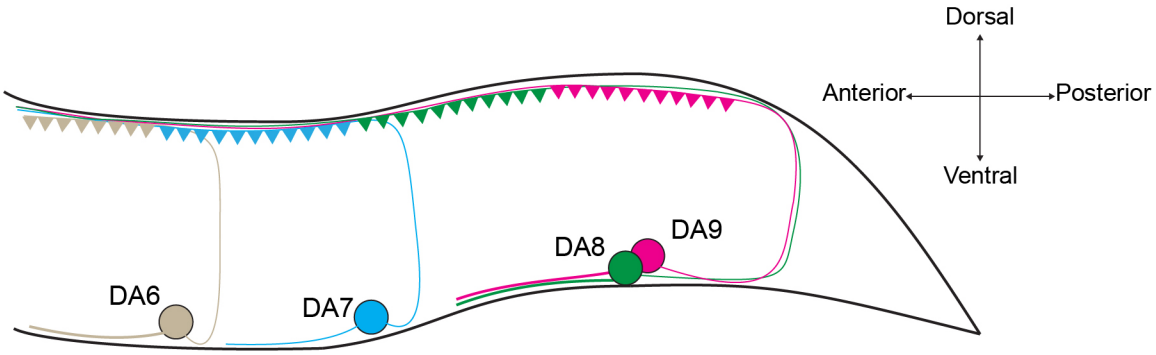

Figure 2. Schematic of synaptic tiling in DA motor neurons of *C. elegans.*

Schematic of the tiled innervation of the posterior DAs (DA6-9). Synapses of each DA neuron is represented with triangles. Synaptic domains of each DA neuron do not overlap with the synaptic domain of its neighbouring neuron. DA cell bodies are represented with circles. Axons and dendrites are represented with lines.

1.5 Neuromuscular junctions of *C. elegans*

The synapses and neuromuscular junctions of *C. elegans* are functionally and structurally well-conserved with vertebrates at the level of electron microscopy (Watanabe et al., 2013; White et al., 1976, White et al., 1986). The genes required for nervous system development and synapse formation is also highly conserved among vertebrates and invertebrates (Kurashina et al., 2019). In *C. elegans,* the postsynaptic muscles extend muscle arms/processes to meet the presynaptic neurons to form neuromuscular junctions (Jorgensen and Nonet, 1995) (Figure 1). This suggests that both neurons and muscles may utilize spatial and specificity cues for proper synapse formation and possibly synapse pattern formation of neuromuscular junctions.

1.6 UNC-4 Homeodomain protein

1.6.1 Homeodomain proteins

Homeodomain proteins are a class of transcription factors that contain a ~60 amino acid DNA binding domain called the homeodomain, which bind to a conserved DNA sequence of 180 nucleotides called the homeobox to regulate gene expression (McGinnis et al., 1984; Scott et al., 1989). These homeodomain proteins, such as Ultrabithorax and Antennapedia*,* were originally identified in *Drosophila*, where mutations in these genes caused developmental abnormalities called 'homeotic' transformations, in which one part of the animal body develops in place of another body part, and are required for the determination of segmental identity of *Drosophila* (Lewis, 1978; Gehring et al., 1984). Mutations in the *Ultrabithorax* gene in *Drosophila* transforms the metathoracic (the hindmost division of the thorax) and first abdominal segments into mesothoracic (the middle division of the thorax) segments (Lewis, 1978). Loss-of-function mutations in the *Antennapedia* gene results in ectopic formation of antennae in place of legs

(Regulski et al., 1985). Hox genes are a subcategory within the homeobox genes that regulate and establish the segmental identity along the anterior-posterior body axis (McGinnis and Krumlauf, 1992; Pearson et al., 2005). While not all homeobox genes are hox genes, many of the homeodomain containing homeobox genes are evolutionarily conserved and are required for the development of organs (Burglin, 2011). For example, the *Iroquois*-related homeobox genes *Irx1, -2, -3, -4,* and *-5* are required for the development of the patterning and development of the heart in mice (Christoffels et al., 2000). Homeobox genes are also intimately involved in the development of the nervous system (Vollmer and Clerc, 1998; Muhr et al., 2001). For example, the *islet* homeobox gene in *Drosophila* is required for the proper axon guidance of the ISNb motor neurons that innervate the ventrolateral body wall muscles (Thor et al., 1997).

1.6.2 The roles of UNC-4 in neuronal development

The homeobox transcription factor UNC-4 has been identified as a neuronal cell fate determinant in *C. elegans* to specify A-type cholinergic motor neurons by repressing the B-type gene expression in DA and VA neurons (Miller and Niemeyer, 1995; Winnier et al., 1999). Loss of *unc-4* or *unc-37* causes ectopic expression of the B-type specific genes such as *del-5* and *acr-5* in A-type neurons (Winnier et al., 1999; Kratsios et al., 2011; Kerk et al., 2017). This repression of B-type gene expression requires the physical interaction between UNC-4 and with the Groucho-like corepressor UNC-37 (Winnier et al., 1999; Von Stetina et al., 2006). In *Drosophila*, a recent study has identified the role of Unc-4 to promote cholinergic fate and inhibit GABAergic fate, and control axonal projection (Lacin et al., 2020), suggesting a conserved role of *unc-4* in neuronal specification. The mammalian ortholog of UNC-4, UNCX, has been identified to regulate the proliferation and survival of neural progenitors in the olfactory sensory neurons (Sammeta et al., 2010). It is not clear if UNCX functions in mice to specify the

olfactory sensory neurons, as the loss of other neuronal cell fate determinants results in apoptosis in the neurons (Cheng et al., 2003; Kadkhodaei et al., 2009).

Besides the roles of *unc-4* in neurodevelopment, its mouse homolog UNCX is known to be involved in the generation of the somites, which give rise to skeletal elements of the vertebral column. Loss of Uncx in mice causes axial skeleton and rib defects, in which the neural arches of the vertebra and proximal ribs do not form (Mansouri et al., 2000; Leitges et al., 2000). In addition to the spinal cord, hindbrain, forebrain, and the somites, Uncx is also found to be expressed in the kidneys where they may play an important role in the development of the kidneys (Mansouri et al., 1997).

The roles of *unc*-4 and *unc-37* in the neuronal wiring of some cholinergic motor neuron classes have also been identified in *C. elegans*. In wildtype animals, VA motor neurons receive presynaptic input from the AVA interneuron (White et al., 1986) however, in the loss of function mutants of *unc-4* or *unc-37,* the AVB interneuron, which normally innervates VB motor neurons, innervates the VA motor neurons instead of AVA, likely due to the partial cell fate transformation of the A-type motor neurons to that of B-type (White et al., 1992; Miller et al., 1992; Pflugrad, et al., 1997; Winnier et al., 1999; Von Stetina et al., 2007). In DB motor neurons, ectopic *unc-4* expression can cause reverse axonal anterior-posterior polarity, in which B-class motor neurons which normally extend their axons posteriorly now extend their axons anteriorly, similar to those of DA neurons (Esmaeili et al., 2002).

1.7 UNC-37/Groucho

unc-37 encodes the ortholog of Groucho/TLE (Transducin-Like Enhancer of split). Groucho/TLE are a group of transcriptional corepressors that are heavily involved in regulating

development including organogenesis (Gasperowicz and Otto, 2005). For example, the Groucho corepressor TLE1 functions in combination with Hesx1 homeodomain transcription factor to repress a transcriptional activator Prop-1 for proper pituitary development (Dasen et al., 2001). Groucho corepressors cannot bind DNA directly to repress transcription but can regulate transcription by physical interaction with transcription factors (Buscarlet and Stifani, 2007). Groucho proteins contain a highly conserved glutamine-rich domain and tryptophan-aspartic acid repeat (WDR) domain which is essential for the physical interaction with transcription factors that contain engrailed-homology 1 (eh1) domains (Buscarlet and Stifani, 2007). Groucho proteins inhibit transcription by inhibiting the RNA polymerase II complex or by recruiting histone deacetylase complexes to remodel chromatin (Calvo et al., 2001; Buscarlet and Stifani, 2007)

unc-37 is ubiquitously expressed and is essential for development, as null mutant mutants produce inviable embryos (McKim et al., 1992; Miller et al., 1993; Pflugrad et al., 1997). *unc-37* is involved in many developmental processes including the regulation of seam cell development (Xia et al., 2007), specification of the uterine muscles (Miller and Okkema, 2011), and controlling the sex-specific apoptosis in male-specific CEM neurons (Peden et al., 2007). In A-type neurons, UNC-37 binds to UNC-4 via the physical interaction between the fifth WD repeat of UNC-37 and the eh1 and C-terminus of UNC-4 (Pflugrad et al., 1997; Winnier et al., 1999).

1.8 Thesis Objective

The goal of this thesis is to uncover the novel roles of cell fate determinants in synaptic pattern formation. Due to the limitations listed above, we have little understanding in the roles of neuronal cell fate determinants at the level of neuronal connectivity. To address this, we use tiled

synaptic innervation of the DA- class cholinergic motor neurons as a system. Specifically, we address following questions:

1. Do *unc-4* and *unc-37* mutant animals have proper tiled synaptic innervation?

2. Are the cell fates of DA8 and DA9 affected in *unc-4* and *unc-37* mutant animals?

3. What are the spatial and temporal requirements of *unc-4* and *unc-37* in regulating synaptic tiling?

4. Do *unc-4* and *unc-37* function in the same genetic pathway as *plx-1*?

5. What functions downstream of *unc-4* to regulate synaptic tiling?

Chapter 2: Materials and Methods

2.1 Visualizing the synaptic tiling between DA8 and DA9 neurons

2.1.1 *mizIs3* marker system

To visualize the tiled synaptic innervation of two DA-class neurons, DA8 and DA9, we have created a transgenic marker strain which utilises the ZIF-1/ZF1 degradation system (Armenti et al., 2014) to degrade GFP::RAB-3 tagged with ZF1 only in DA9 neurons (Fig. 1F). We expressed RAB-3 fused with GFPnovo2, a codon-optimized brighter variant of GFP (Hendi and Mizumoto, 2018), and ZF1 under the *unc-4* promoter. In DA9 we expressed mCherry::RAB-3 and ZIF-1 from the *mig-13* promoter. ZIF-1 expressed in DA9 leads GFPnovo2::ZF1::RAB-3 fusion protein to the ubiquitin mediated protein degradation. This provides clear color separation of the DA8 synapses labeled with GFP and DA9 synapses labeled with only mCherry.

2.1.2 Laser scanning confocal microscopy

Confocal microscopy is an imaging technique that increases optical resolution by using a pinhole to block out-of-focus light from beyond the imaging plane. Similar to traditional fluorescent microscopy, fluorophores (Ex. GFP, mCherry, BFP) are illuminated using a laser with a specific excitation filter to produce a specific wavelength of light (excitation wavelength), which is absorbed by the respective fluorophore (see below) which then emits a longer wavelength of light (emission wavelength). The emission wavelength is filtered through a dichroic mirror and detected using a detector.

Images of fluorescently tagged fusion proteins were captured in live *C. elegans* using a Zeiss LSM800 Airyscan confocal microscope (Carl Zeiss, Germany) with oil immersion lens 63x magnification (Carl Zeiss, Germany). Worms were immobilized on 2.5% agarose pad using

a mixture of 7.5 mM levamisole (Sigma-Aldrich) and 0.225M BDM (2,3-butanedione monoxime) (Sigma-Aldrich). Laser wavelengths of 383nm, 488nm, and 587nm were used to excite BFP, GFP, and mCherry signals, respectively. Images were analyzed with Zen software (Carl Zeiss). 20-26 Z-stacks of 0.43μm thickness were taken for each animal to encompass the cell bodies, axons and synapses of the DA8 and DA9 neurons. The cell bodies of DA8 and DA9 were determined by the presence of GFP and mCherry in the cell bodies, respectively. The definition of each parameter is as follows (Mizumoto and Shen, 2013; Chen et al., 2018): DA8/DA9 overlap: the distance between the most anterior DA9 synapse and the most posterior Middle L4 larval stage animals (judged by the stereotyped shape of the developing vulva) were used for quantification.

2. 2 Nematode strain culture

2.2.1 General Maintenance of *C. elegans*

All strains were cultured in the nematode growth medium (NGM) as described previously (Brenner, 1974). Bristol N2 strain was used as a wildtype reference. Maintenance is performed using stereomicroscopes (ZEISS Stemi 305 and ZEISS SteREO Discovery.V8). Unless particularly noted, all strains were grown at room temperature (~22°C) for analysis. Mutant strains used in this study are listed in Table 1.

Table 1. List of strains used in this work

strain	genotype	transgene used	Used in Figure(s)
VC2010	N2 (wildtype reference)		Figure 1-4, 8-11
CB120	*unc-4 (e120) II*		Figure 1-3, 8-12
NC37	*unc-4 (e2322) II*		Figure 4, 10
NC168	*unc-4 (e26) II*		Figure 2

CB262	*unc-37 (e262) I*		Figure 1, 3, 8-10
ZB1748	*plx-1 (nc36) IV*		Figure 8
VC1039	*ceh-12 (gk436) I*		Figure 12
UJ98	*mizIs1*	*Pitr-1::mCherry::rab-3, Pitr-1::zf1-GFPnovo2::CAAX, Pvha-6::zif-1, Podr-1::RFP*	Figure 3
UJ124	*mizIs3*	*Punc-4::zf1-GFPnovo2::rab-3, Pmig-13::zif-1, Pmig-13::mCherry::rab-3, Podr-1::RFP*	Figure 1, 2, 4, 6-8, 12
TV11417	*wyIs320*	*Pitr-1::plx-1::GFP, Pmig-13::mCherry::rab-3, Podr-1::GFP*	Figure 10
OH12389	*hdIs1*	*Punc-53::GFP + rol-6(su1006)*	Figure 3
UJ1333	*mizEx396*	*Punc-129DB::his-24::mCherry, Punc-4c::his-24::GFPnovo2, Podr-1::GFP*	Figure 3
NC972	*wdEx419*	*Pacr-16::GFP + rol-6(su1006)*	Figure 3
UJ1415	*mizEx410*	*Punc-4c::his-24::mCherry, Podr-1::GFP*	Figure 3
OH12887	*otIs476*	*Pglr-4::TagRFP*	Figure 3
	hdIs1;mizEx410		Figure 3
	wdEx419;mizEx410		Figure 3
UJ1141	*mizEx362*	*Pplx-1::GFP, Punc-4::his-24::mCherry, Podr-1::GFP*	Figure 9
UJ1144	*mizEx365*	*Prap-2::GFP, Punc-4::his-24::mCherry, Podr-1::GFP*	Figure 9
UJ1331	*mizIs3;mizEx394*	*Punc-4c::ceh-12, Punc-4c::his-24::GFPnovo2, Podr-1::GFP*	Figure 12
UJ1332	*mizIs3;mizEx395*	*Punc-4c::ceh-12, Punc-4c::his-24::GFPnovo2, Podr-1::GFP*	Figure 12
UJ1413	*mizIs3;mizEx408*	*Punc-4c::unc-55A, Punc-4c::his-24::GFPnovo2, Podr-1::GFP*	Figure 12
UJ1414	*mizIs3;mizEx409*	*Punc-4c::unc-55A, Punc-4c::his-24::GFPnovo2, Podr-1::GFP*	Figure 12
UJ1133	*mizSi3 IV*	*Punc-4c::TIR1*	Figure 5-7

UJ1017	*unc-4 (miz40Ins[unc-4::AID::BFP]) II*		Figure 5-7
UJ1013	*unc-37 (miz36Ins[unc-37::AID::BFP]) I*		Figure 5-7
UJ703	*unc-4(e120);mizIs3*		Figure 1, 2, 8, 12
UJ1411	*unc-4(e26);mizIs3*		Figure 2
UJ1279	*unc-4(e2322);mizIs3*		Figure 4
UJ968	*unc-37(e262);mizIs3*		Figure 1, 8
UJ1329	*plx-1(nc36);mizIs3*		Figure 8
UJ1282	*unc-37(e262);unc-4(e120);mizIs3*		Figure 1
UJ913	*unc-4(e120);plx-1(nc36);mizIs3*		Figure 8
UJ821	*unc-37(e262);plx-1(nc36);mizIs3*		Figure 8
UJ1337	*ceh-12(gk436);mizIs3*		Figure 12
	ceh-12(gk436);unc-4;mizIs3		Figure 12
UJ1159	*unc-4(miz40Ins);mizSi3;mizIs3*		Figure 5-7
UJ1161	*unc-37(miz36Ins);mizSi3;mizIs3*		Figure 5-7
UJ1031	*unc-37(e262);mizIs1*		Figure 3
UJ1449	*unc-4(e120);wyIs320*		Figure 3, 10
UJ1447	*unc-4(e2322);wyIs320*		Figure 10
UJ1314	*unc-37(e262);wyIs320*		Figure 3, 10
UJ1453	*unc-4(e120);hdIs1;mizEx410*		Figure 3
UJ1455	*unc-37(e262);hdIs1;mizEx410*		Figure 3
UJ1352	*unc-4(e120);mizEx396*		Figure 3
UJ1334	*unc-37(e262);mizEx396*		Figure 3
	unc-4(e120);wdEx419;mizEx410		Figure 3
	unc-37(e262);wdEx419;mizEx410		Figure 3
UJ1348	*unc-4(e120);mizEx362*		Figure 9
UJ1345	*unc-37(e262);mizEx362*		Figure 9

UJ1350	*unc-4(e120);mizEx365*	Figure 9
UJ1346	*unc-37(e262);mizEx365*	Figure 9

2.2.2 DNA Extraction and Genotyping of Strains

Genotypes of some mutant strains were determined by visible phenotypes such as, uncoordinated locomotion (Unc), and/or were confirmed using polymerase chain reaction (PCR) followed by gel electrophoresis. The genotyping primers used in this study are listed in Table 2.

To extract DNA from a given plate, worms are collected from a starved plate with 100 µL M9 buffer into an empty PCR tube. The supernatant was removed and 20 µL of lysis buffer (50 mM KCl, 10 mM Tris pH 8.3, 2.5 mM MgCl2, 0.45% NP-40, 0.45% Tween-20, 20 mg/mL proteinase K) was added. The mixture was vortexed, incubated at 65°C for 1.5 hours, and 95°C for 15 minutes, for proteinase K inactivation. The lysis product would be used as a template for PCR amplification (DreamTaq DNA Polymerase, Thermo Fisher Scientific).

Table 2. Genotyping primers used in this study.

Genotype	Forward	reverse (outside deletion)	reverse (inside deletion) OR enzyme
plx-1(nc36)	**cttcgagagccccctcattcttaatg**	**ccggcacacgttaaactagtgctaccg**	
ceh-12(gk436)	**gatcccagaggcaagaatga**	**cgaaccgcattcagcagtga**	**cctaccgtagtcgcttatgaa**
unc-4(miz40Ins)	**agtctccccctcttccaacc**	**gaaccgtgccctccattgg**	**catggaaggaaccgtggac**
unc-37(miz36Ins)	**agtctccccctcttccaacc**	**gaaccgtgccctccattgg**	**catggaaggaaccgtggac**

2.2.3 Using *unc-4(e2322)* temperature sensitive mutants to determine that temporal requirement of *unc-4* in synaptic tiling

unc-4(e2322) mutant variant contains a point mutation (L121F) causing a Leucine to Phenylalanine change at amino acid position 121 (Winnier et al., 1999). This point mutation resides in the homeodomain of UNC-4 which is required for the DNA binding to homeobox DNA sequence. This mutation is permissive at 16°C and restrictive at 25°C allowing for temporal control of UNC-4 function.

unc-4(e2322) mutants were cultured at 16°C or 25°C for one generation. Experimental animals were transferred from 16°C and 25°C to 25°C and 16°C, respectively, at the first larval stage (L1) post hatching for the post-embryonic and embryonic knockdown of UNC-4. Animals that were not transferred were quantified as controls. To test the embryonic requirement of *unc-4*, *unc-4(e2322)* mutant animals were transferred at the fourth larval stage (L4) to continue developing at 25°C (restrictive temperature) until they lay eggs. Newly hatched L1 larval stage animals were transferred to 16°C (permissive temperature) until L4 larval stage where we then visualized the synaptic tiling of DA8 and DA9 neurons. To test the post-embryonic requirement of *unc-4*, *unc-4(e2322)* mutant animals were transferred at L4 larval stage to continue developing at 16°C (permissive temperature) until they lay eggs. Newly hatched L1 larval stage animals were transferred to 25°C (restrictive temperature) until L4 larval stage where we then visualized the synaptic tiling of DA8 and DA9 neurons.

2.2.4 Spatial and temporal degradation of UNC-4 and UNC-37 using the auxin-inducible degron (AID) system

A plant specific degradation system called the auxin-inducible degron (AID) system was introduced in non-plant cells to allow for inducible degradation of AID-tagged proteins in the presence of a plant F-box ubiquitin ligase, TIR1, and a plant hormone, auxin (Nishimura et al., 2009). The AID system was introduced in *C. elegans* by Zhang et al., 2015. AID-tagged proteins, in the presence of TIR1 and auxin, are degraded through ubiquitination and subsequent transport to the proteasome. The degradation of AID-tagged proteins is spatially controlled by restricting the expression of TIR1 using cell-specific promoters, and temporally controlled by controlling the timing of auxin supplementation. Using CRISPR-Cas9 mediated genome editing we have created the conditional mutant alleles, *unc-4(miz40[unc-4::AID::BFP])* and *unc-37(miz36[unc-37::AID::BFP])*, where the AID degron fused to BFP were inserted into the 3' end of the *unc-4* and *unc-37* genomic loci, respectively. Using CRISPR-Cas9 mediated genome editing, *mizSi3[Punc-4c::TIR1]* to generate the experimental strains. The synthetic auxin, α-Napthaleneacetic Acid (K-NAA), was dissolved in dH_2O to prepare a 400 mM stock solution which was stored at 4°C for up to one month. The 400 mM stock solution was diluted in M9 to a working 4 mM concentration. NGM (Nematode Growth Medium) agar plates with fully grown OP50 bacterial lawn were coated with 1000 µL of the 4 mM auxin solution and were allowed to dry overnight at room temperature. To induce protein degradation, experimental animals were transferred onto the auxin-coated plates and kept at room temperature. As a control, animals were transferred onto M9-coated plates without K-NAA.

2.3 Transgenic Strains

2.3.1 Plasmid Construction

C. elegans expression clones were made in a derivative of pPD49.26 (A. Fire), the pSM vector (a kind gift from S. McCarroll and C. I. Bargmann). *ceh-12, unc-55A* cDNA clones were obtained by RT-PCR from N2 mRNA using Superscript III First-strand synthesis system and Phusion High- Fidelity DNA Polymerase (Thermo Fisher Scientific). See Table 3 for cDNA primer sequence.

Table 3. cDNA primer sequence

Gene	Forward	reverse (outside deletion)
ceh-12	cttcttcttccaaaaagtgaaaggcgcgccatgatgttttcctcaataga	caatcaacttcctcttcttgaggtaccatggtattgatatctgagctc
unc-55A	cttcttcttccaaaaagtgaaaggcgcgccatgcaggatggctcatcagg	caactaccttccagaaattagggtaccatggtattgatatctgagctc

2.3.2 CRISPR-Cas9 mediated genome editing to create transgenic mutant animals (*miz36, miz40, mizSi3)*

To tag the endogenous *unc-4* and *unc-37* locus with AID fused to BFP at the C-terminus we used CRISPR-Cas9 genome editing. The repair template contained a 500bp length upstream homology arm and a 500bp length downstream homology arm from the desired insertion site, cloned from *C. elegans* gDNA.

The repair template plasmid, *unc-4* and *unc-37* sgRNA plasmids, and a Cas9 plasmid (Addgene #46168) (Friedland et al., 2013) were co-injected into young adults. Candidate genome-edited animals were screened based on G418 resistance and uniform expression of P*myo-2::GFP* in the pharynx (Au et al., 2019). The selection cassette was then excised by

injecting Cre recombinase plasmid (pDD104, Addgene #47551). The junctions between *unc-4/unc-37* coding sequence and AID as well as AID and BFP were confirmed by Sanger sequencing.

We targeted the Chr V: 8,643,066 intergenic region which is known to be resistant to the germline silencing (Frokjaer-Jensen et al., 2014), for single copy insertion using CRISPR-Cas9 mediated genome editing (Obinata et al., 2018). We inserted a single copy of Punc-4c::TIR1-loxP-Pmyo-2:::GFP + NeoR-loxP into the oxTi365 MosSCI site. Candidate genome-edited animals were screened based on G418 resistance and uniform expression of P*myo-2::GFP* in the pharynx as described previously (Au et al., 2019). The selection cassette was then excised by injecting Cre recombinase plasmid (pDD104, Addgene #47551).

2.4 Quantification and statistical analysis

Confocal images were examined using ZEISS ZEN Imaging Software (blue edition), coarse quantification of promoter reporter expression in DA8 and DA9 neurons was using ZEISS Axioplan 2 universal microscope.

Data was analyzed using Prism7 (GraphPad Software, USA). We applied one-way ANOVA method with posthoc Tukey's multiple comparisons test for comparison among more than three parallel groups with multiple plotting points, and Chi-square test (with Yates' continuity corrected) for comparison between two binary data groups. Data were plotted with error bars representing standard errors of mean (SEM). *, ** and *** represent P value <0.05, <0.01 and <0.001 respectively

3. Results

3.1 *unc-4/Hox* and *unc-37/Groucho* is required for the synaptic patterning of DA8 and DA9 neurons.

3.1.1 Visualization of synaptic tiling in DA8 and DA9 neurons

The *C. elegans* cholinergic motor neurons, DA, DB, VA, VB, and AS, have tiled synaptic innervation in which neurons of the same class form synapses onto the body wall muscle with adjacent motor neurons in a complete but non-overlapping manner while their axons (White et al., 1978; Mizumoto and Shen, 2013; Chen et al., 2018) (Figure 3A). This tiled patterning occurs only between neurons within the same neuronal class, possibly suggesting a mechanism for respective neuronal classes to govern tiled innervation.

We have previously visualized the tiled synaptic patterning of 2 DA-class cholinergic motor neurons, DA8 and DA9, utilizing the combination of the *unc-4* promoter (DA and VA-specific) to drive the expression of GFP-tagged RAB-3, a presynaptic vesicle marker, and the *mig-13* promoter (DA9 and VA12-specific) to drive the expression of mCherry tagged RAB-3 (Mizumoto and Shen, 2013; Chen et al., 2018). Using this marker strain, we can observe DA8 synapses labeled with GFP and DA9 synapses co-labeled with GFP and mCherry. However, to cleanly distinguish DA8 synapses and DA9 synapses, we have created a new transgenic marker strain which utilises the ZIF-1/ZF1 degradation system (Armenti et al., 2014) to degrade GFP::RAB-3 tagged with ZF1 only in DA9 neurons (Fig. 3F). We expressed RAB-3 fused with GFPnovo2, a codon-optimized brighter variant of GFP (Hendi and Mizumoto, 2018), and ZF1 under the *unc-4* promoter. In DA9 we expressed RAB-3 tagged with mCherry and ZIF-1 from the *mig-13* promoter. ZIF-1 expressed in DA9 leads to GFPnovo2::ZF1::RAB-3 to the ubiquitin

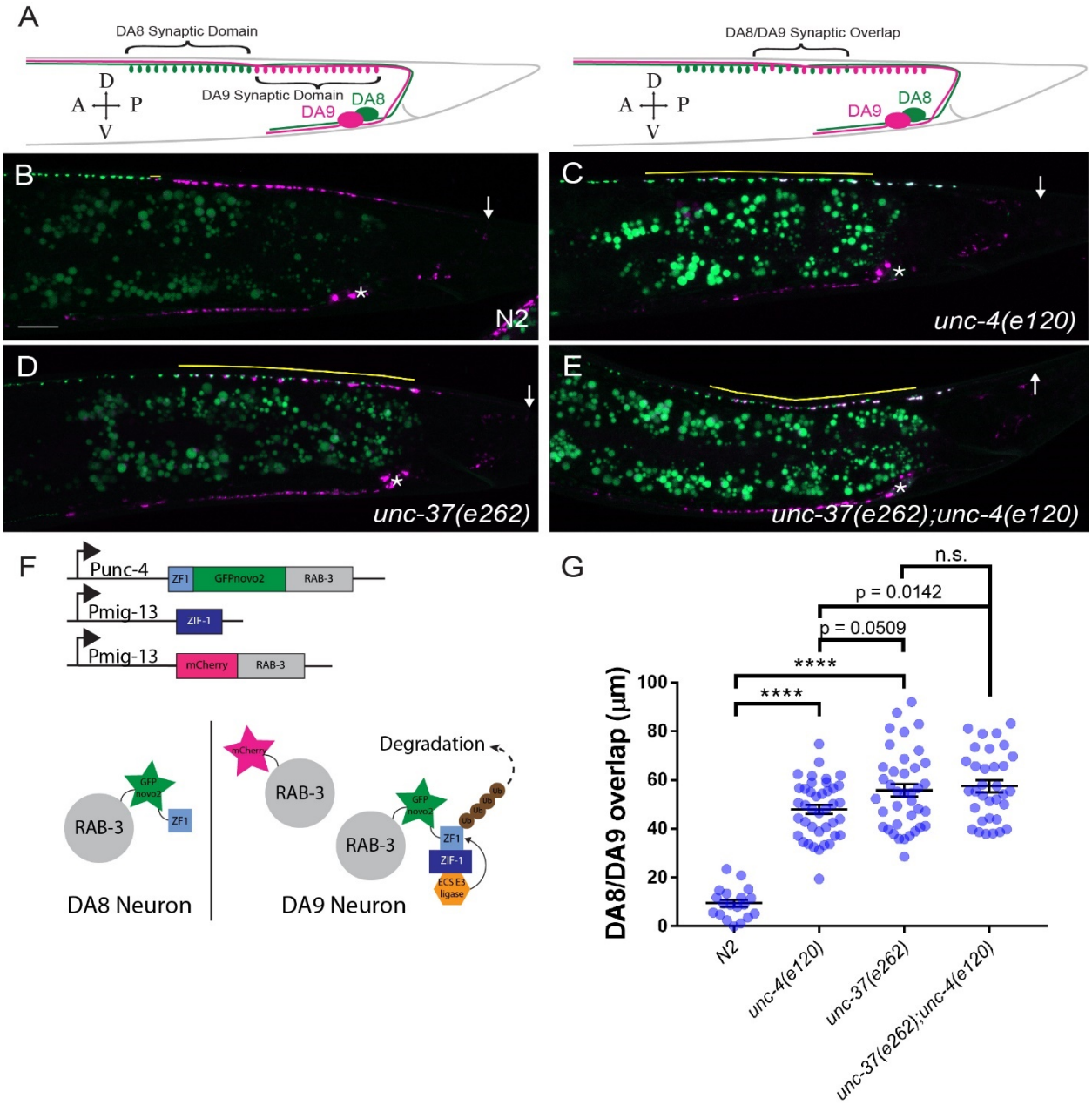

Figure 3. *unc-4* and *unc-37* are required for tiled synaptic innervation of DA8 and DA9 neurons.

(A) Schematic of the tiled innervation between DA8 and DA9 neurons visualized by the *mizIs3* marker. (B-G) Representative images of synaptic tiling in N2 (B), *unc-4(e120)* (C), *unc-37(e262)* (D), and *unc-37(e262);unc-4(e120)* (E). Synaptic overlap between the DA8 and DA9 synaptic domains are highlighted with a yellow line. Asterisks: DA9 cell body. Arrows: dorsal commissure of DA9. Puncta at the ventral side of the worms are from the VA12 neuron that is also labeled with *Pmig-13. Scale* bar: 10µm. (F) Schematic of *mizIs3* marker system. (G) Quantification of overlap of DA8 and DA9 synaptic domains in *unc-4* and *unc-37* mutants. Each dot represents a single animal. Black bars indicate ± SEM. n.s.: not significant; ****: p<0.0001

mediated protein degradation. This provides clear separation of the DA8 synapses labeled with GFP and DA9 synapses labeled with only mCherry. As previously described, wildtype animals do not show significant overlap between the synaptic domains of DA8 and DA9 neurons with the new marker system (Figure 3B) (Mizumoto and Shen, 2013; Chen et al., 2018).

3.1.2 *unc-4* and *unc-37* are required for tiled synaptic innervation of DA8 and DA9

In A-type motor neurons (DAs and VAs), UNC-4/Hox and UNC-37/Groucho form a transcriptional repressor complex to repress the expression of B-type specific genes such as *del-1* and *acr-5* (Winnier et al., 1999; Esmaeili et al., 2002). *unc-4* is exclusively expressed in DAs and VAs, while *unc-37* is ubiquitously expressed (Miller et al., 1992; Miller and Niemeyer 1995; Esmaeili et al., 2002; Pflugrad et al.,1997). To determine if the UNC-4-UNC-37 transcriptional repressor complex that specify A-type neuronal fates are required for the synaptic patterning in DA neurons, we examined the synaptic tiling of DA8 and DA9 neurons in *unc-4* mutant animals. In *unc-4* mutants, we found a striking degree of overlap between the DA8 and DA9 synaptic domains (Figure 3C). Previously we showed that physical contact between the DA8 and DA9 axons are required to maintain proper tiled synaptic innervation (Mizumoto and Shen, 2013). Interestingly, we found that in *unc-4* mutants the degradation of GFP::RAB-3 was incomplete in DA9 neurons (Figure 3C). We also noticed that the mCherry::RAB-3 expression in DA9 neurons was dimmer compared to wildtype animals. *unc-4* likely decreases the overall strength from the DA9-specific P*mig-13,* which causes the DA9 synapses to be marked by both GFP and mCherry, rather than mCherry alone. (See Section 3.2.2). We found that in *unc-4* mutant animals, a small portion (approximately ~20%) showed defasciculation phenotype of the DA8 and DA9 axons. We have excluded these animals from our quantifications. To determine if *unc-37* is also

required for the synaptic patterning of DA neurons, we use the hypomorphic mutant allele of *unc-37(e262)* which causes a histidine to tyrosine substitution at the amino acid position 539, in the 5th WD repeat (Pflugrad et al., 1997) Null mutants of *unc-37* cause sterility and inviable embryos and have pleiotropic phenotypes (McKim et al., 1992; Miller et al., 1993; Pflugrad et al., 1997). The *e262* mutation causes the backwards locomotion defect that is observed in all *unc-37* mutants but are otherwise fertile and morphologically normal (Pflugrad et al., 1997). The *e262* mutation is a specific mutation that perturbs the structure necessary for UNC-4 activity (Pflugrad et al., 1997). In *unc-37(e262)* mutant animals, we also observed overlap between the DA8 and DA9 synaptic domains to a similar degree as *unc-4* mutant animals, indicating that *unc-37* is also required for synaptic tiling (Figure 3D). Furthermore, *unc-4(e120)* did not enhance the synaptic tiling defects of *unc-37* (Figure 3E and 3G), suggesting that *unc-4* and *unc-37* function in the same genetic pathway. We did observe that *unc-37* single mutants exhibit slightly larger overlaps between the DA8 and DA9 synaptic domains but were statistically not significant compared with *unc-4* mutants (Figure 3G). As a ubiquitously expressed transcriptional co-repressor with multiple binding partners, it is possible that *unc-37* also functions with other transcription factors to regulate the tiled patterning of DA8 and DA9. Consistently, we noticed an increase in defasciculation defects in the *unc-37;unc-4* double mutants, suggesting *unc-37* may have an additive role with *unc-4* in fasciculation. We excluded animals with fasciculation defects from our quantification.

UNC-37 has been shown to physically interact with UNC-4 via its carboxy-terminal Engrailed-like repressor domain (eh1) and this physical interaction is necessary for the repression of B-type specific genes (Winnier et al., 1999). To test if *unc-4* and *unc-37* function together in tiled synaptic innervation, we examined an *unc-4* mutant allele (e26) which has a

missense mutation in the eh1 domain and has been previously shown to disrupt the physical interaction between UNC-4 and UNC-37 (Winnier et al., 1999). Consistent with the null allele *unc-4(e120)* and *unc-37* mutant animals, we observed large overlaps between the DA8 and DA9 synaptic domains in *unc-4(e26)* mutant animals (Figure 4), suggesting that the formation and physical interaction of the UNC-4/UNC-37 repression complex is required for proper tiled innervation.

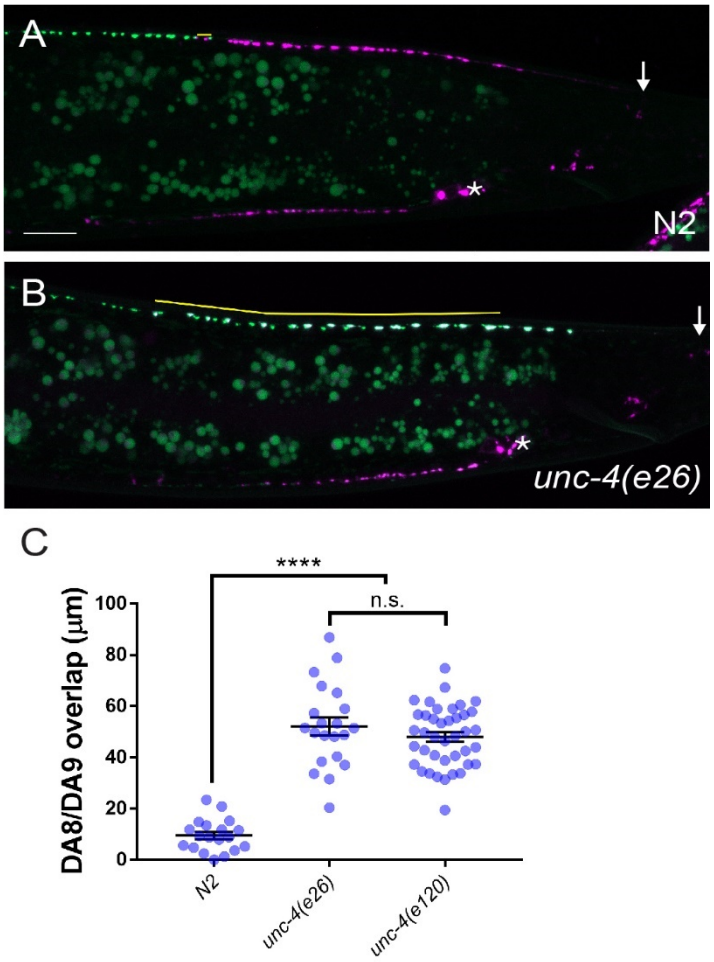

Figure 4. *unc-4(e26)* mutant animals have severe synaptic tiling defects.

(A and B) Representative image of synaptic tiling in N2 (A) and *unc-4(e26)* mutant (B) animals. (C) (H) Quantification of overlap of DA8 and DA9 synaptic domains. Each dot represents a single animal. Black bars indicate ± SEM. n.s.: not significant; ****:p<0.0001

3.2 Determining the cell fate defects of DA8 and DA9 in *unc-4* and *unc-37* mutants

3.2.1 DA8 and DA9 cell fates are largely unaffected in *unc-4* and *unc-37* mutants

VA and VB cholinergic neurons share the same cellular lineage and are sister cells, whereas DA and DB neurons have distinct cellular lineages with DB neurons having unique origins from each other (Sulston 1983; Sulston et al., 1983). As *unc-4* and *unc-37* determine the A-type motor neuron fates by repressing B-type specific genes (Kerk et al., 2017;), it is possible that the synaptic tiling defects of *unc-4* and *unc-37* mutant animals may be a secondary defect of the neuronal cell fate transformation in DA8 and DA9 neurons. We therefore examined the A-type neuronal identity of DA8 and DA9 with three DA/DB cell fate markers: P*unc-53::GFP* expressed in DA and AS cholinergic motor neurons, P*acr-16::GFP* and a truncated P*unc-129db::GFP* expressed in DB neurons (Kratsios et al., 2015; Kerk et al., 2017; Kratsios et al., 2017; Winnier et al., 1999; Kratsios et al., 2011). In wildtype animals, DA8 and DA9 expressed P*unc-53::GFP* but not P*acr-16::GFP* or P*unc-129db::GFP* (Figure 5A-C). In the *unc-4(e120)* and *unc-37* mutant animals DA8 and DA9 neurons expressed P*unc-53::GFP,* suggesting that DA neurons still retain their A-type identity (Figure 5A). Interestingly, in the *unc-4* or *unc-37* mutants we did not observe ectopic expression of the DB marker P*unc-129db::GFP* promoter (Figure 5B). However, we observed a minor increase in the ectopic expression of the DB marker P*acr-16::GFP* in DA**9** neurons but not DA8 neurons in both *unc-4* and *unc-37* mutant animals (Figure 5C). While the slight increase in ectopic expression is statistically significant, the ectopic expression of P*acr-16::GFP* is not fully penetrant (~10% in *unc-4* mutants and ~25% in *unc-37* mutants), unlike the complete penetrant effect on synaptic tiling. Together, our data suggests that

DA8 and DA9 retain A-type cell identity in *unc-4* and *unc-37* mutants and are not fully transformed to B-type neurons.

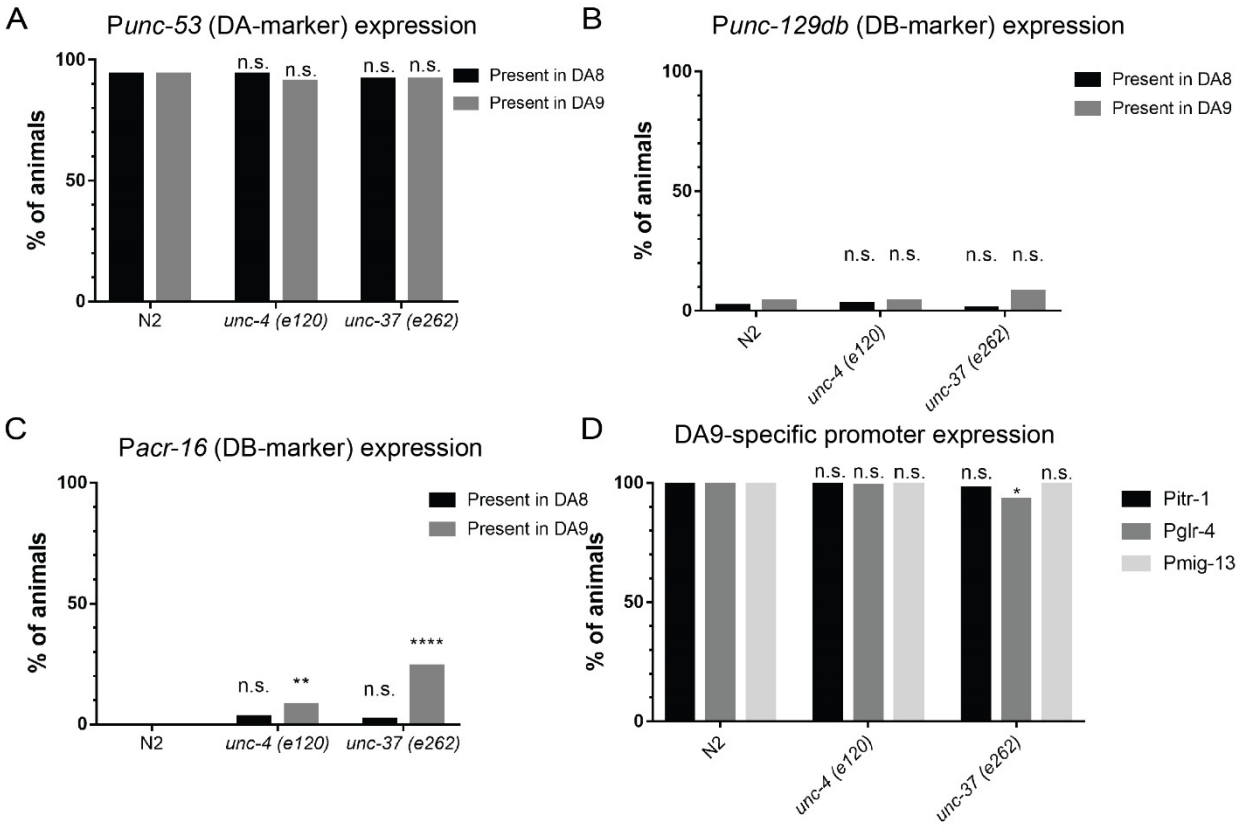

Figure 5. Loss of *unc-4* or *unc-37* does not cause significant cell fate defects in DA neurons.

The expression of A- and B-type chlolinergic markers is largely unaffected in *unc-4* and *unc-37* mutant animals. (A-C) Quantification (percentage of animals) is provided with black bars representing expression in DA8 neurons, while grey bars represent expression in DA9 neurons. (A) A-type cholinergic marker (*unc-53*). (B) B-type cholinergic marker (*unc-129db*). (C) B-type cholinergic marker (*acr-16*). (D) Quantification (percentage of animals) is provided with black bars representing the expression of P*itr-1*, dark grey bars representing the expression of P*glr-4*, and light grey bars representing the expression of P*mig-13* in DA9 neurons. n.s.: not significant; * : $p<0.05$; ** : $p<0.001$; **** : $p<0.0001$

3.2.2 DA9-specific cell markers are largely unaffected in *unc-4* and *unc-37* mutants

We further tested the identity of DA9 neurons using DA9-specific markers, P*mig-13*, P*glr-4*, and P*itr-1* (Klassen and Shen, 2007; Kratsios et al., 2017). In wildtype animals, these DA9 markers are expressed in DA9 at full penetrance (Figure 5D). In *unc-4* mutant animals, we observed complete expression from the *itr-1, mig-13,* and *glr-4* promoters in DA9 neurons (Figure 5D). We note that the expression from the *mig-13* promoter judged by the expression of *Pmig-13::mCherry*::*rab-3* in *mizIs3* was weaker in many *unc-4* animals (Figure 5B). Likewise, the expression from the *itr-1* promoter was weaker in *unc-4* mutant animals (Figure 12B). In *unc-37* mutant animals, we found that the expression of these DA9 specific markers were mostly unaffected, with a small number of animals lacking P*glr-4* expression in the DA9 neuron.

Together we concluded that the cell fate defects of DA8 and DA9 in *unc-4* and *unc-37* mutants were very minor, if any, and therefore are unlikely to underlie the high penetrance of synaptic tiling defects observed in these mutants.

3.3 Testing the spatial and temporal requirement of *unc-4* and *unc-37*

3.3.1 *unc-4* functions post-embryonically to regulate synaptic tiling

Recent works have revealed the roles of neuronal cell fate determinants in postmitotic neurons to maintain neuronal identity (Kratsios et al., 2011; Deneris and Hobert, 2014; Alqadah et al., 2015; (see review, Hobert, 2016)). For example, the *C. elegans* POU homeobox gene *unc-86* and its mouse ortholog *Brn3a* are required for the maintenance of glutamatergic identity and medial habenular neurons, respectively (Serrano-Saiz et al., 2018). Given that *unc-4* and *unc-37* mutants do not exhibit drastic cell fate defects in DA8 and DA9, we sought to test their temporal requirement in synaptic tiling.

DA neurons are born and complete their development during embryogenesis (Sulston et al., 1983), and the tiled synaptic innervation of DA8 and DA9 is observed at early L1 larval stage (Mizumoto and Shen, 2013). We used a reversible temperature-sensitive mutant of *unc-4(e2322ts)* (Miller et al., 1992; Winnier et al., 1999) to dissect the temporal requirement of *unc-4*. At the permissive temperature (16°C), *unc-4(e2322ts)* mutants exhibited minimal synaptic tiling defects that was not significantly different from wildtype grown at 16°C (Figure 6C). As expected, at the restrictive temperature (25°C), *unc-4(e2322ts)* mutants showed severe synaptic tiling defects at similar degree to *unc-4(null)* mutants grown at 25°C (Figure 6D), suggesting that the function of *unc-4(e2322ts)* is almost completely abolished at the restrictive temperature. We then determined if *unc-4* functions embryonically or post-embryonically to regulate synaptic tiling by either up-shifting or down-shifting the growth temperature at early L1 larval stage when the development of DA neurons have already completed (Figure 6A). Interestingly, we observed severe synaptic tiling defects when the growth temperature of *unc-4(e2322ts)* mutant animals were up-shifted from 16°C to 25°C at L1 larval stage (Figure 6F). Conversely, we found that the temperature down-shift from 25°C to 16°C at L1 larval stage resulted in minimal synaptic tiling defects (Figure 6G). This result strongly suggests that *unc-4* required is not required for synaptic tiling during the embryonic stage when DA8 and DA9 cell fates are determined, and that *unc-4* is required post-embryonically for synaptic tiling of DA8 and DA9.

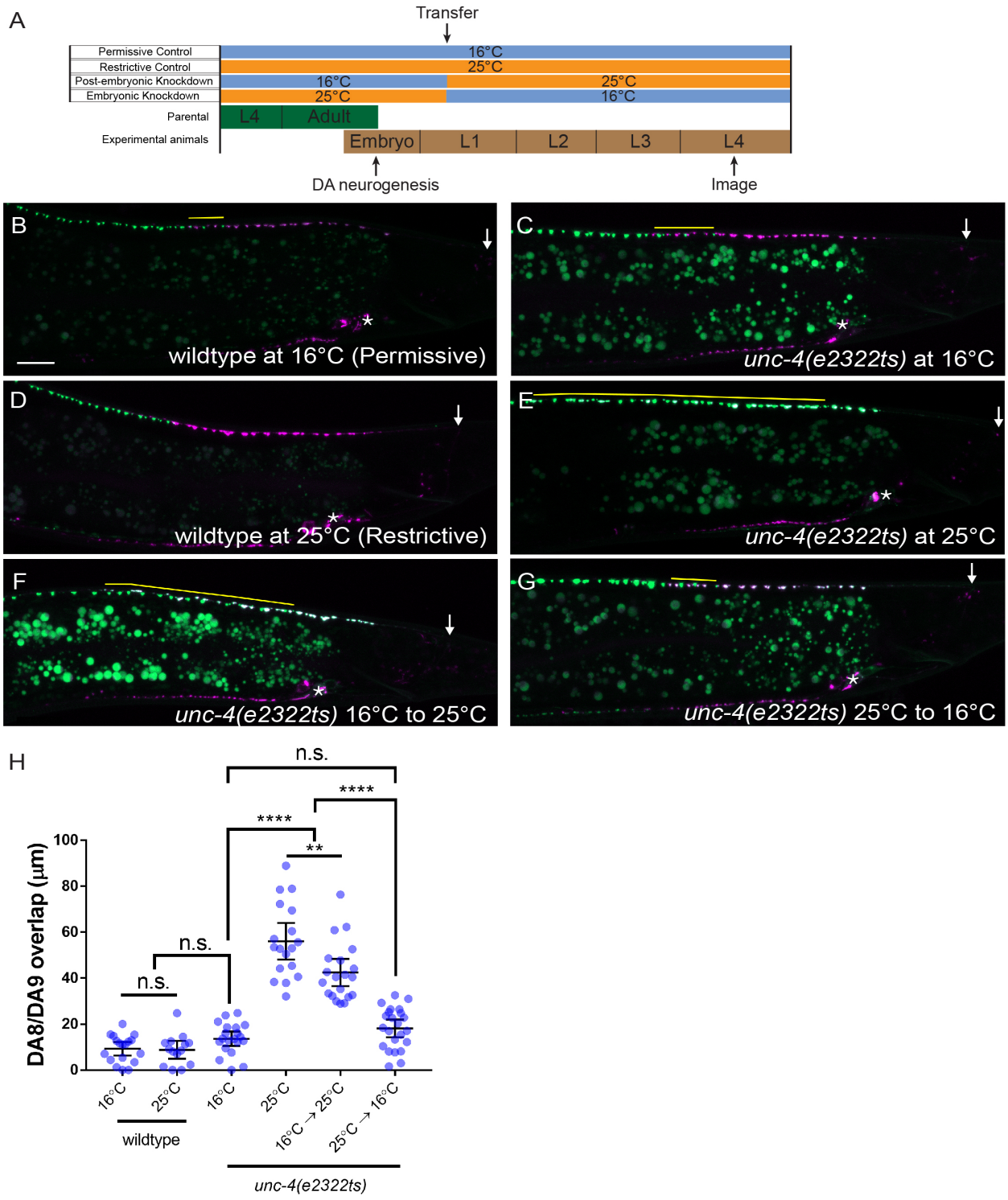

Figure 6. *unc-4* functions postembryonically for the synaptic tiling of DA8 and DA9 neurons.

(A) Schematic of the temperature shift assay (B-G) Representative images of synaptic tiling in N2 at 16°C (A), N2 at 25°C (B), *unc-4(e2322)* at 16°C (C), *unc-4(e2322)* at 25°C (D), *unc-4(e2322)* 16°C to 25°C (E), and *unc-4(e2322)* 25°C to 16°C (F). Synaptic overlap between the

DA8 and DA9 synaptic domains are highlighted with a yellow line. Asterisks: DA9 cell body. Arrows: dorsal commissure of DA9. Scale bar: 10μm. (G) Quantification of overlap of DA8 and DA9 synaptic domains. Each dot represents a single animal. Black bars indicate ± SEM. n.s.: not significant; **: p<0.01; ****:p<0.0001.

3.3.2 Using Auxin-mediated degradation to elucidate the temporal requirement of *unc-4* and *unc-37*

To further verify the post-embryonic role of *unc-4* in synaptic tiling, we utilized Auxin-inducible degron (AID) system to knockdown UNC-4 in a spatiotemporally controlled manner. A plant-specific auxin-dependent ubiquitin ligase TIR1 mediates the degradation of AID tagged protein in an auxin-dependent manner (Dharmasiri et al., 2005; Kepinski and Leyser, 2005; Zhang et al., 2015). Using CRISPR/Cas9-mediated genome editing, we tagged endogenous *unc-4* with an AID-degron tag fused to BFP at the 3' end of the *unc-4* ORF (*miz40[unc-4::AID::BFP])* (Figure 7B). Consistent with the previous studies, we observed expression of UNC-4::AID::BFP fusion protein in the nuclei of DA and VA neurons (Fox et al., 2005; Miller and Niemeyer, 1995), including the DA8 and DA9 neurons (Figure 8A). We then crossed *unc-4(miz40)* with *mizSi3 (Punc-4c::TIR1)*, a transgene that expresses TIR1 specifically in DA neurons (Figure 7A). With this strain, we could knock-down endogenous *unc-4* specifically in DA neurons upon auxin treatment. *unc-4(miz40);mizSi3* animals did not exhibit uncoordinated locomotion phenotype or synaptic tiling defects (Figure 9A) in the absence of auxin, suggesting that the UNC-4::AID::BFP fusion protein expressed from the endogenous locus is fully

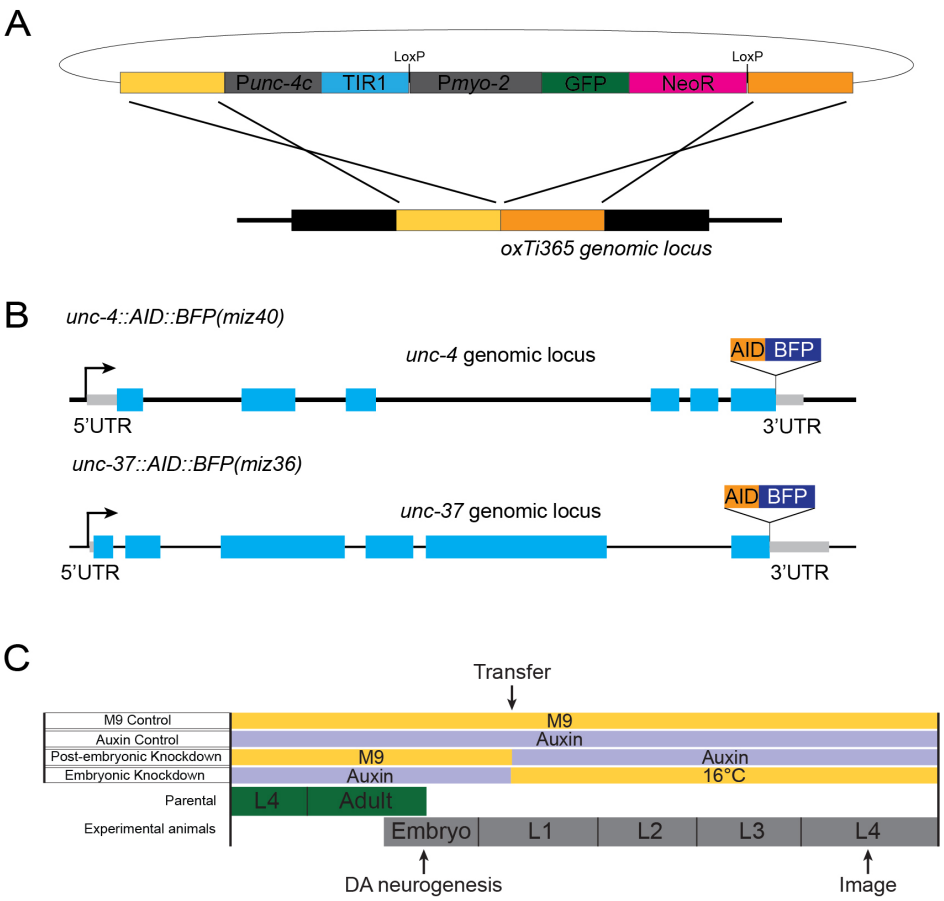

Figure 7. Schematics of AID genomics and AID assay.

(A) Schematic of the oxTi365 locus used to insert a single copy of P*unc-4c::TIR1* with selection cassette using CRISPR/Cas9 mediated genome editing. (B) Schematic of genome-edited *unc-4* (top) and *unc-37* (bottom) locus. (C) Schematic of auxin treatment in AID assay.

functional. When *unc-4(miz40);mizSi3* animals were grown on the plate with the water-soluble synthetic auxin analog (K-NAA) (Martinez et al., 2020) dissolved in M9, we observed loss of UNC-4::AID::BFP signal from DA neurons but not from VA neurons (Figure 8B), suggesting the successful DA-specific knockdown of UNC-4. Using this system, we first tested the DA-specific continuous UNC-4 knockdown (embryonic and post-embryonic) by growing L4 larval stage animals on K-NAA plates and observing their progeny at L4 larval stage, and observed a large synaptic tiling defect between DA8 and DA9 synaptic domains (Figure 8B). Notably, as the degradation of UNC-4 is specific to DA neurons, this result suggests that *unc-4* is required cell autonomously in DA neurons for tiled synaptic innervation.

We then conducted embryonic UNC-4 knockdown in DA neurons by growing L4 larval stage animals on K-NAA plates and rescued their progenies at early L1 larval stage to the control M9-containing NGM plates (Figure 7C). For post-embryonic UNC-4 knockdown in DA neurons, we transferred early L1 larval stage animals from the control NGM plates to the K-NAA-containing NGM plates and let them grow until L4 larval stage (Figure 7C). Consistent with the temperature shift experiments using *unc-4(e2322ts)* mutant animals, we did not observe synaptic tiling defects when UNC-4 is embryonically knocked down (Figure 9C). Post-embryonic UNC-4 knockdown resulted in significant synaptic tiling defects (Figure 9D). From these experiments we conclude UNC-4 functions post-embryonically in DA neurons to maintain tiled synaptic innervation.

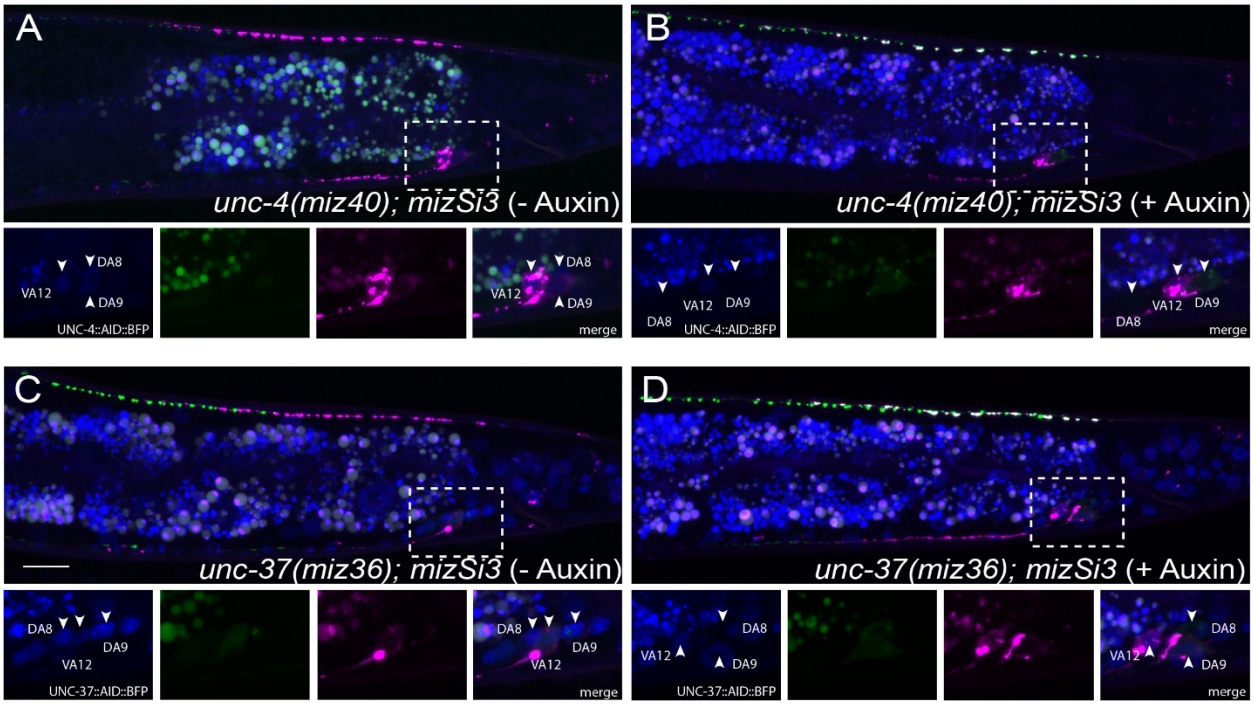

Figure 8. Auxin treatment induces degradation of AID-degron tagged UNC-4 and UNC-37.

(A) Representative image of *unc-4(miz40)* grown on M9 control plates. UNC-4::AID::BFP is expressed in A-type cholinergic motor neurons. (B) Representative image of *unc-4(miz40)* grown on K-NAA auxin plates. UNC-4::AID::BFP is degraded in DA neurons but not VA neurons. (C) Representative image of *unc-37(miz36)* grown on M9 control plates. UNC-37::AID::BFP is

ubiquitously expressed and is also expressed in A-type cholinergic motor neurons. (D) Representative image of *unc-37(miz36)* grown on K-NAA auxin plates. UNC-37::AID::BFP is only degraded in DA neurons.

We next asked if *unc-37,* which functions with *unc-4* in DA cell fate specification, is also required post-embryonically in synaptic tiling. Using a similar method as above, we generated an AID-BFP tagged allele of *unc-37(miz36)* (Figure 7B). *unc-37(miz36*) animals also did not exhibit uncoordinated locomotion or synaptic tiling defects (Figure 9F), indicating that UNC-37::AID::BFP fusion protein is functional. Similar to UNC-4::AID::BFP, we observed DA neuron-specific loss of BFP signal (Figure 8C and D) and severe synaptic tiling defects in *unc-37(miz36); mizSi3(Punc-4c::TIR1)* animals grown continuously on the K-NAA NGM plate (Figure 9G). Strikingly, unlike *unc-4* which is only required post-embryonically, we found that both embryonic and post-embryonic degradation of UNC-37::AID::BFP in DA neurons caused synaptic tiling defects to a similar degree to the continuous (embryonic and post-embryonic) knockdown (Figure 9H-J). *unc-37* is therefore required for the establishment of the synaptic tiling between DA8 and DA9 during embryogenesis as well as for its maintenance during post-embryonic development. This result suggests that *unc-37* may function with another transcription factor during embryonic development to determine the synaptic tiling border.

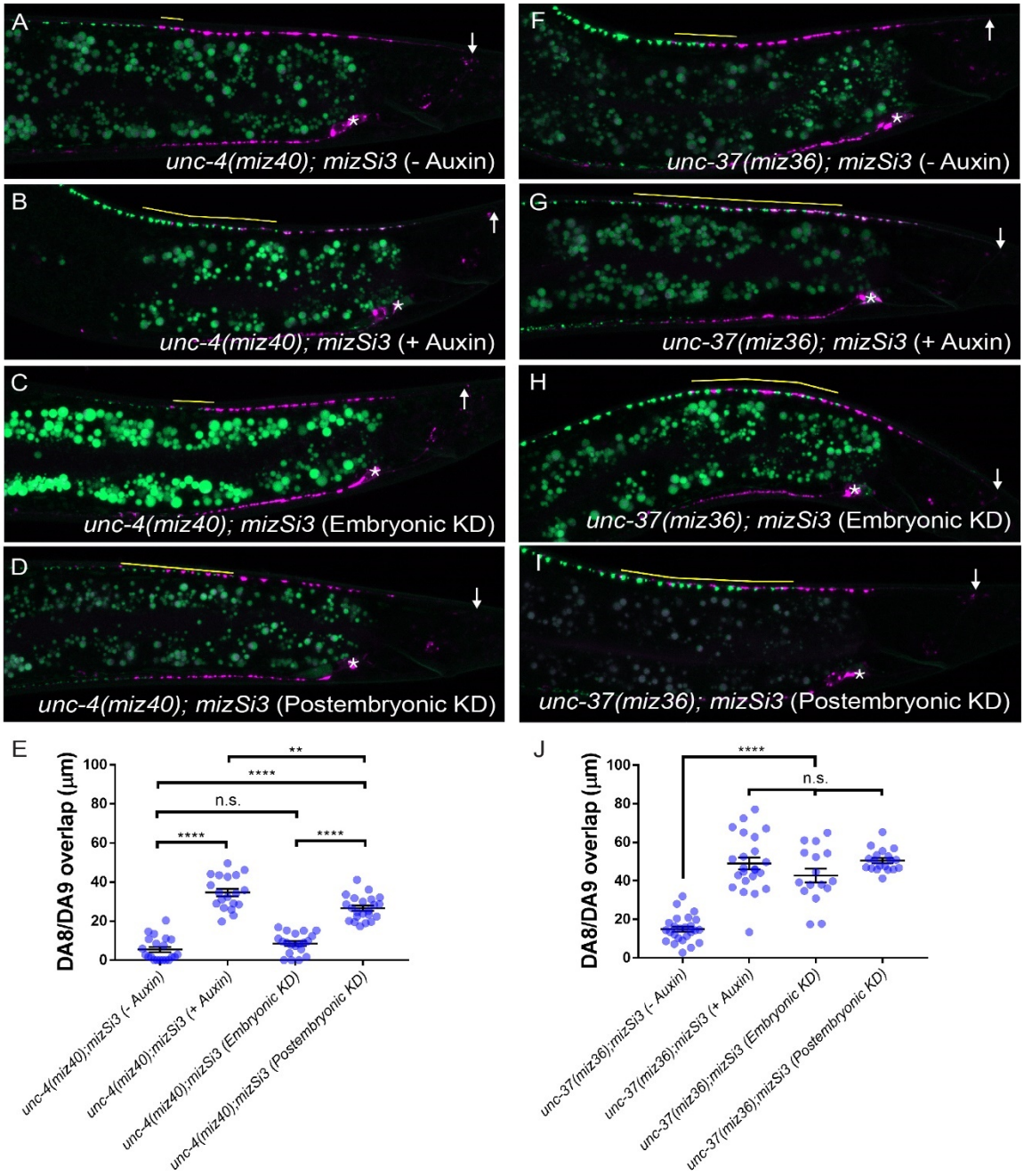

Figure 9. *unc-4* functions postembryonically while *unc-37* is required embryonically and postembryonically to regulate tiled synaptic innervation

(A-D) Representative images of synaptic tiling in *unc-4(miz40)* (-Auxin) (A), *unc-4(miz40)* (+Auxin) (B), *unc-4(miz40)* (Embryonic Degradation) (C), *unc-4(miz40)* (Postembryonic Degradation) (D). (E) Quantification of overlap of DA8 and DA9 synaptic domains in the *miz40* mutant animals. (F-I) Representative images of synaptic tiling in *unc-37(miz36)* (-Auxin) (F), *unc-37(miz36)* (+Auxin) (G), *unc-37(miz36)* (Embryonic Degradation) (H), and *unc-37(miz36)* (Postembryonic Degradation) (I). Synaptic overlap between the DA8 and DA9 synaptic domains are highlighted with a yellow line. Asterisks: DA9 cell body. Arrows: dorsal commissure of

DA9. Scale bars: 10μm. (J) Quantification of overlap of DA8 and DA9 synaptic domains in the *miz36* mutant animals. Each dot represents a single animal. Black bars indicate ± SEM. n.s.: not significant; **: p<0.01; ****:p<0.0001

3.4 The relation between *plx-1* signaling cascade and neuronal cell fate determinants

3.4.1 *unc-4* and *unc-37* functions in the same genetic pathway as *plx-1*

We have previously shown that Semaphorin (Sema)-Plexin signaling mediates the synaptic tiling of the DA8 and DA9 (Mizumoto and Shen, 2013; Chen et al., 2018). In the loss of function mutants of *smp-1/SEMA, plx-1/Plexin,* and *rap-2/Rap2A,* DA8 and DA9 show severe synaptic tiling defects (Chen et al., 2018). Since UNC-4 and UNC-37 are transcriptional regulators, it is possible that they regulate synaptic tiling by regulating the expression of Sema-Plexin signaling components. Consistent with this idea, *plx-1* did not enhance the synaptic tiling defects of *unc-4* or *unc-37* (Figure 10E-G). This suggests that both *unc-4* and *unc-37* function in the same genetic pathway as the *plx-1* signaling cascade that mediates synaptic tiling.

3.4.2 *unc-4* and *unc-37* does not regulate the expression of the known *plx-1* pathway

We then tested whether *unc-4* and *unc-37* regulates the expression of the known Sema-Plexin signaling cascade. We have previously identified that *smp-1* and *plx-1* function cell autonomously in DA9 neurons to regulate synaptic tiling (Mizumoto and Shen, 2013), whereas *rap-2* functions in both DA8 and DA9 (Chen et al., 2018). Using reporter strains expressing GFP from the promoters of *plx-1* and *rap-2*, we examined the GFP expression in *unc-4* and *unc-37*

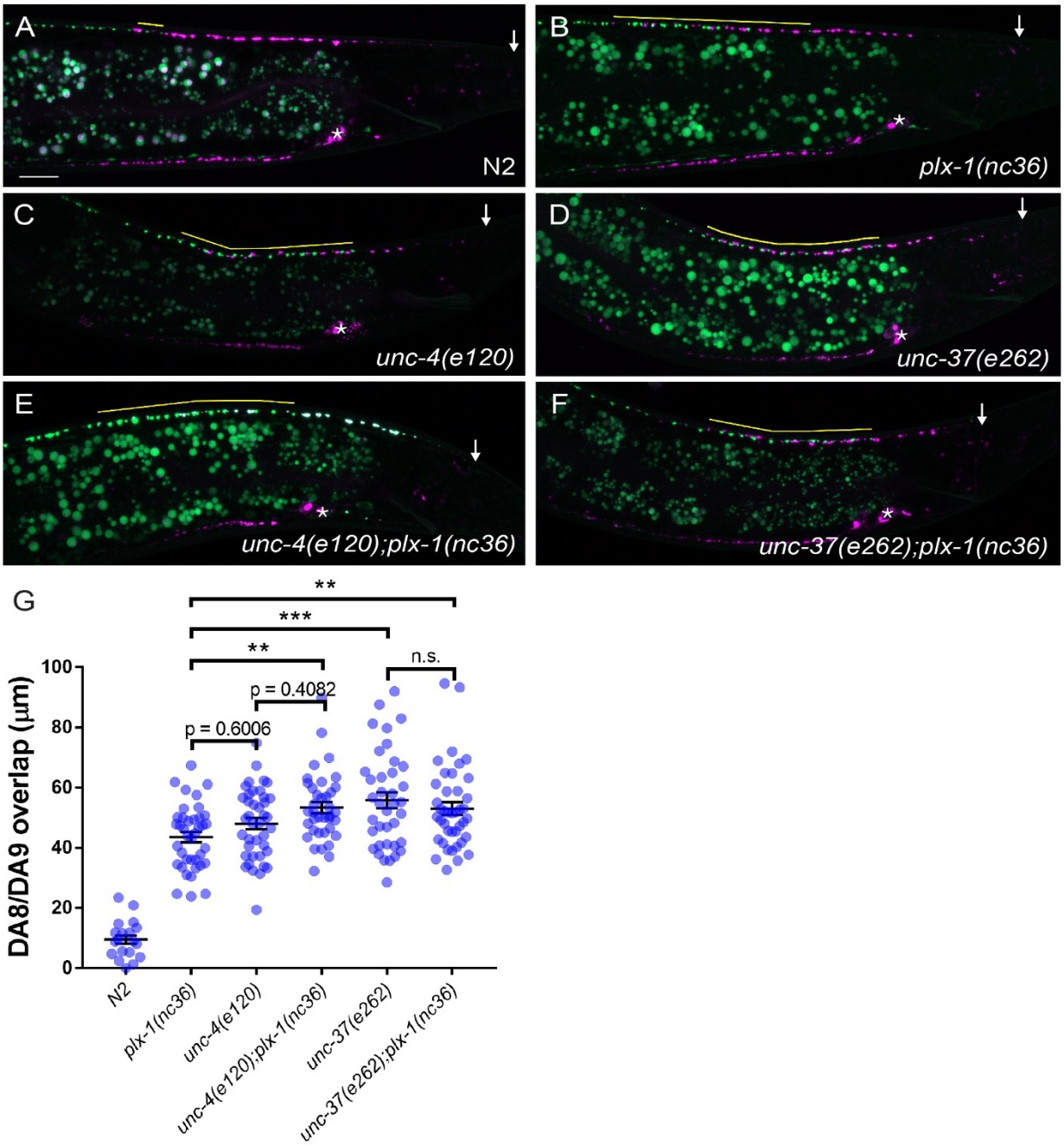

Figure 10. *unc-4* and *unc-37* function in the same genetic pathway as *plx-1*.

(A-F) Representative images of synaptic tiling in N2 (A), *plx-1(nc36)* (B), *unc-4(e120)* (C), *unc-37(e262)* (D), *unc-4(e120);plx-1(nc36)* (E), and *unc-37(e262);plx-1(nc36)* (F). Synaptic overlap between the DA8 and DA9 synaptic domains are highlighted with a yellow line. Asterisks: DA9 cell body. Arrows: dorsal commissure of DA9. Scale bar: 10µm. (H) Quantification of overlap of DA8 and DA9 synaptic domains. Each dot represents a single animal. Black bars indicate ± SEM. n.s.: not significant; **: p<0.01; ***:p<0.001

mutants. In wildtype animals, GFP expression from the *plx-1* and *rap-2* promoter was observed in DA8 and DA9 neurons (Figure 11A and B). This is consistent with the findings that *plx-1* functions in DA9 neurons and *rap-2* functions in both DA8 and DA9 to regulate synaptic tiling (Mizumoto and Shen, 2013; Chen et al., 2018). In *unc-4* and *unc-37* mutant animals, we did not observe a drastic reduction or loss of *plx-1* or *rap-2* expression compared to wildtype animals (Figure 11A' and B'). We observed expression of GFP in the ventral body wall muscles under the *smp-1* promoter which masked the expression from the DA8 and DA9 neurons [data not shown]. While we saw a slight but statistically significant decrease in the number of animals that express *plx-1* in *unc-4* mutant animals, more than 90% of animals still express *plx-1* in DA9. It is therefore unlikely to be the direct cause of the synaptic tiling defects in *unc-4* mutants, as we see a complete penetrant effect on synaptic tiling.

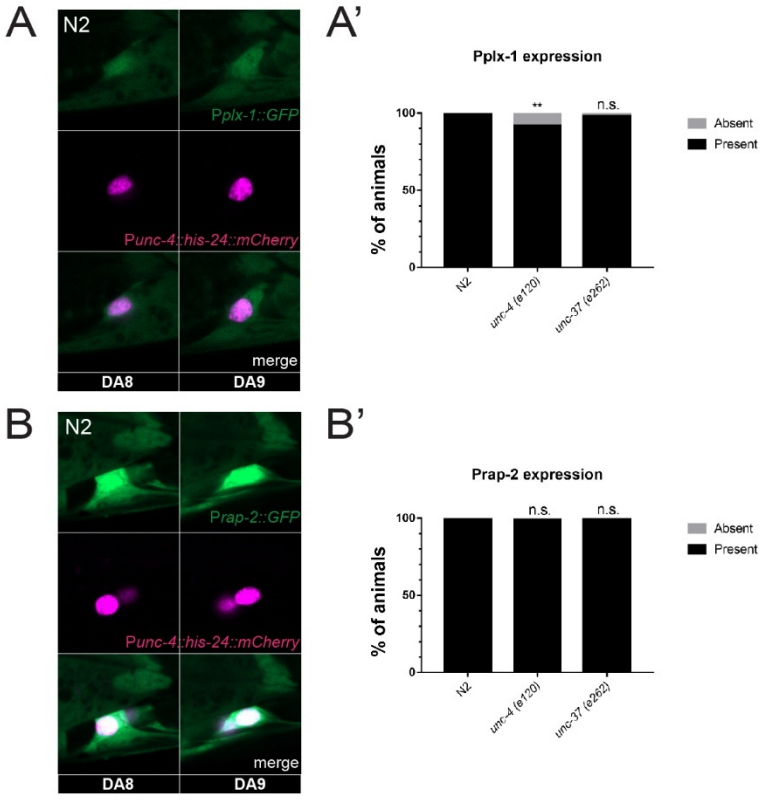

Figure 11. *unc-4* and *unc-37* does not regulate the expression of *plx-1* or *rap-2.*

(A) Representative image of P*plx-1::GFP* expression in DA8 and DA9 neurons in wildtype animals. P*unc-4c::his-24::mCherry* was used as an internal control to verify the DA8 and DA9 cell bodies. (A') Quantification of P*plx-1::GFP* expression in N2, *unc-4,* and *unc-37* mutant animals. (B) Representative image of P*rap-2::GFP* expression in DA8 and DA9 neurons in wildtype animals. P*unc-4c::his-24::mCherry* was used as an internal control to verify the DA8 and DA9 cell bodies. (B') Quantification of P*rap-2::GFP* expression in N2, *unc-4,* and *unc-37* mutant animals.

While we have shown that *smp-1* is required and sufficient in DA9 for synaptic tiling (Mizumoto and Shen, 2013), our P*smp-1::his-24::GFP* construct did not label DA neurons consistently, possibly because the 2kb promoter sequence was not sufficient to reproduce the endogenous *smp-1* expression. Therefore, we indirectly tested if *smp-1* expression is altered in the *unc-4* and *unc-37* mutants by examining PLX-1::GFP localization on the DA9 axon. PLX-1::GFP shows patched localization at the anterior edge of the DA9 synaptic domain in a *smp-1*-dependent manner (Figure 12A) (Mizumoto and Shen; 2013). In *smp-1* mutants, PLX-1::GFP is diffused throughout the axon. If the synaptic tiling defects of *unc-4* and *unc-37* mutants is due to the loss of *smp-1* expression, we would see diffused PLX-1::GFP localization. However, in *unc-4* and *unc-37* mutants, we observed the patched localization of PLX-1::GFP in the DA9 axon (Figure 12B and C), suggesting that *smp-1* functions properly in the *unc-37* mutant background. The PLX-1::GFP localization in *unc-4(e120)* mutants were dim as the transgene utilizes the *itr-1* promoter to express PLX-1::GFP in DA9 neurons (Figure 12B). Therefore, we tested the PLX-1 localization in the temperature sensitive *unc-4(e2322)* mutant animals at the restrictive temperature (25°C). We found that in *unc-4(e2322)* mutant animals grown at the restrictive temperature, the strength of expression from the *itr-1* promoter is indistinguishable from wildtype animals (Figure 12D). We observed patched localization of PLX-1::GFP in the DA9 axon, suggesting that *smp-1* functions properly in the *unc-4* mutant background. Additionally, expression of known Sema/Plexin signaling components' cDNA (*smp-1, plx-1 rap-2* or *mig-15*) under the DA neurons-specific promoter (*unc-4c*) did not rescue the synaptic tiling defects of *unc-4* and *unc-37* mutants (data not shown). It is therefore unlikely that *unc-4* and *unc-37* regulate synaptic tiling via expression of the known Sema-Plexin signaling components.

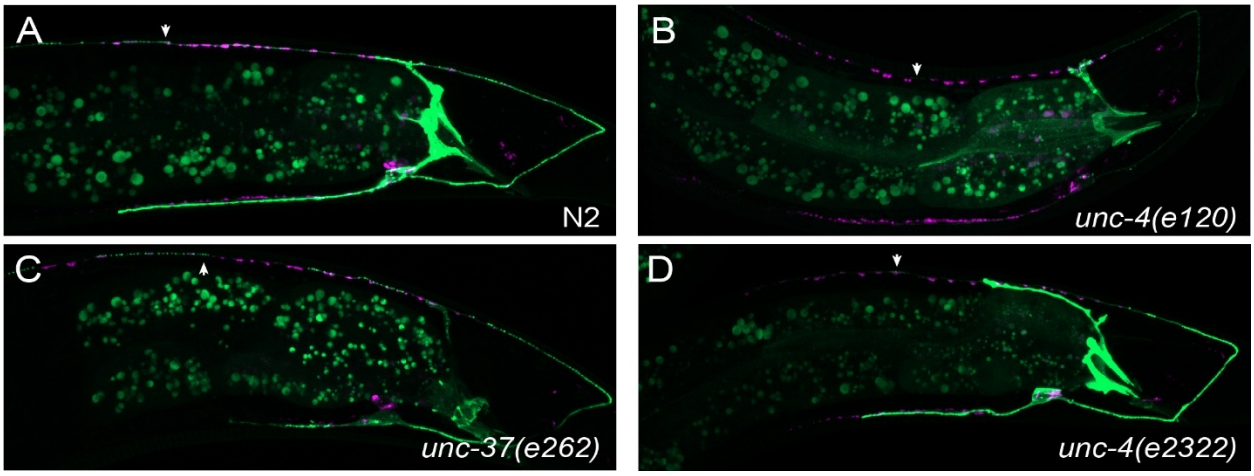

Figure 12. PLX-1 localization is unaffected in *unc-4* and *unc-37* mutant animals.

(A-D) Representative image of PLX-1::GFP in N2 (A) *unc-4(e120)* mutant (B) *unc-37* mutant (C) *unc-4(e2322)* mutant (D) animals. PLX-1 localizes anteriorly to the DA9 synaptic domain (represented by the arrow) to regulate the tiling border between DA8 and DA9 (Mizumoto and Shen, 2013).

While PLX-1::GFP localization was unaffected in *unc-4(e120), unc-4(e2322),* and *unc-37* mutants, the presynaptic marker, mCherry::RAB-3, was often mislocalized anteriorly to the PLX-1::GFP patch (Figure 12B-D). This is reminiscent to the PLX-1::GFP localization in the mutants of intracellular effectors of PLX-1, *rap-2* and *mig-15* (Chen et al., 2018). In the absence of PLX-1 downstream effectors, the localized PLX-1 at the anterior edge of DA9 synaptic domain cannot locally restrict synapse formation. The normal PLX-1::GFP localization with disrupted synapse patterning suggests that *unc-4* and *unc*-37 regulates the expression of genes that function downstream of PLX-1.

3.5 Identifying possible downstream effectors

3.5.1 *ceh-12* functions downstream of *unc-4*

It has been previously shown that a member of the HB9 family of homeodomain proteins, *ceh-12*, functions downstream of *unc-4* and *unc-37* to specify the synaptic inputs of VA neurons from the AVA interneuron (Von Stetina et al., 2006). UNC-4 and UNC-37 represses the expression of *ceh-12* in A-type motor neurons. Loss of *ceh-12* in *unc-4* and *unc-37* mutant animals partially restored the synaptic and locomotion defects; and the transgenic expression of *ceh-12* in VA neurons was sufficient to induce *unc-4* mutant-like locomotion (Von Stetina et al., 2006). To determine if *ceh-12* also functions downstream of *unc-4* and *unc-37* in regulating tiled synaptic innervation, we first examined the expression of GFP under the *ceh-12* promoter in wildtype and *unc-4* mutant animals. We observed no visible of expression of GFP under the

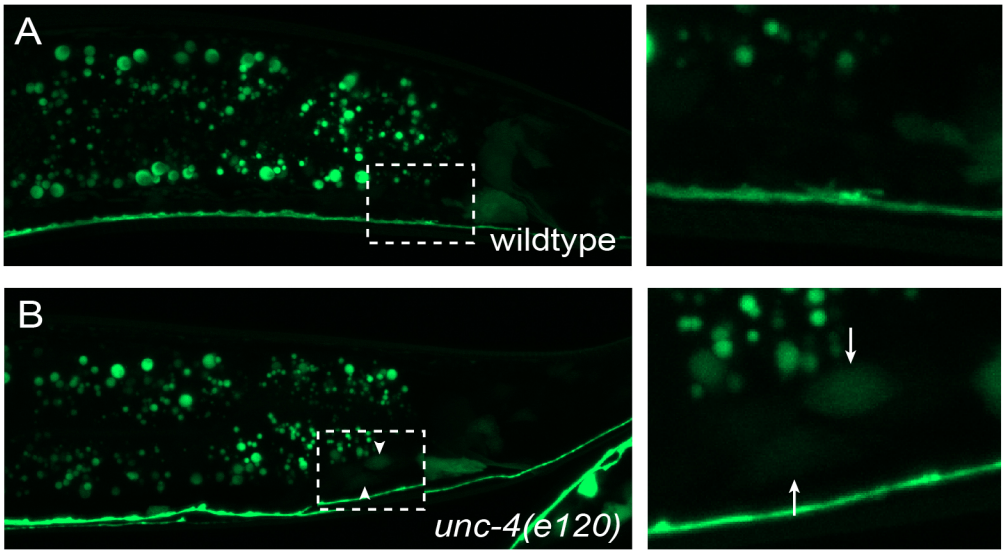

Figure 13. Ectopic expression from the *ceh-12* promoter in DA8 and DA9 neurons in *unc-4* mutants.

(A) Representative image of P*ceh-12::GFP* in wildtype animals. (B) Representative image of P*ceh-12::GFP* in *unc-4(e120)* mutant animals. Ectopic expression of GFP from the *ceh-12* promoter is observed in the cells of the preanal ganglion where DA8 and DA9 cell bodies reside, *unc-4* mutant animals .

ceh-12 promoter in DA8 and DA9 neurons of wildtype animals (Figure 13A). However, in *unc-4* mutants, we observed ectopic expression of P*ceh-12::GFP* in DA8 and DA9 (Figure 13B). This suggests that *unc-4* and *unc-37* functions to repress *ceh-12* expression in the posterior DA neurons. To test if the ectopic expression of *ceh-12* causes synaptic tiling defects, we ectopically expressed *ceh-12* cDNA using the DA neurons-specific promoter (P*unc-4c*) in wildtype animals. We observed significant tiling defects, similar to *unc-4* mutant animals, suggesting that *ceh-12* may also function to regulate tiled synaptic innervation (Figure 14A). To exclude the possibility that the synaptic tiling defects of the *ceh-12* expressing animals is due to the ectopic expression of the cell fate determinants in general, we used the ectopic expression of the A-isoform of *unc-55* cDNA under the truncated *unc-4c* promoter as a control. *unc-55*, an orphan nuclear hormone receptor, is exclusively expressed in VD GABAergic motor neurons and is required for the synaptic specificity and motor neuron traits of VD neurons (Zhou and Walthall, 1998). Ectopic expression of *unc-55A* in DA neurons caused no significant synaptic tiling defects (Figure 14B). Interestingly, we found that the loss of *ceh-12* in *unc-4* mutant backgrounds does not suppress the synaptic tiling defects observed in the single mutants of *unc-4* and *unc-37* (Figure 14E and F). This suggests that there are additional factor(s) which functions in parallel with *ceh-12* under the control of the UNC-4/UNC-37 repressive complex in synaptic tiling (Figure 15). Together, while we cannot conclude that *ceh-12* functions downstream of *unc-4* and *unc-37* in tiled synaptic innervation, it is likely that *ceh-12* functions redundantly with other transcription factors that ultimately control the tiled synaptic innervation in DA neurons.

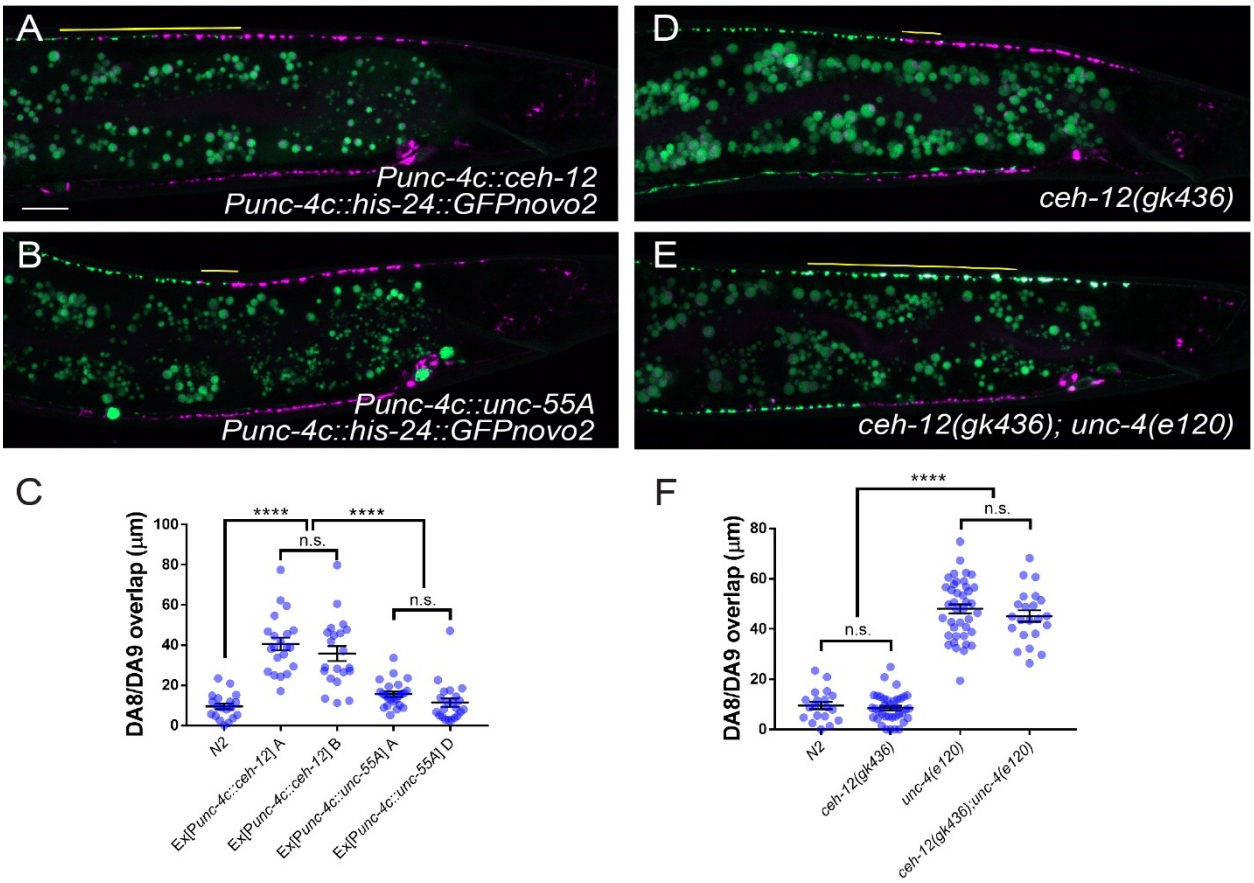

Figure 14. *ceh-12* may function downstream of *unc-4* to regulate tiled synaptic innervation.

(A and B) Representative image of P*ceh-12::GFP* in N2 (A) and *unc-4* mutant (B) animals. (C and D) Representative image of synaptic tiling in ectopic expression of *ceh-12* under the *unc-4c* promoter (C) and *unc-55A* under the *unc-4c* promoter (D). (E) Quantification of overlap of DA8 and DA9 synaptic domains in the transgenic expression lines. Each dot represents a single animal. Black bars indicate ± SEM. n.s.: not significant; ****:p<0.0001 (F and G) Representative image of synaptic tiling in *ceh-12* mutant (F) and *ceh-12; unc-4* mutant (G) animals. (H) Quantification of overlap of DA8 and DA9 synaptic domains. Each dot represents a single animal. Black bars indicate ± SEM. n.s.: not significant; ****:p<0.0001

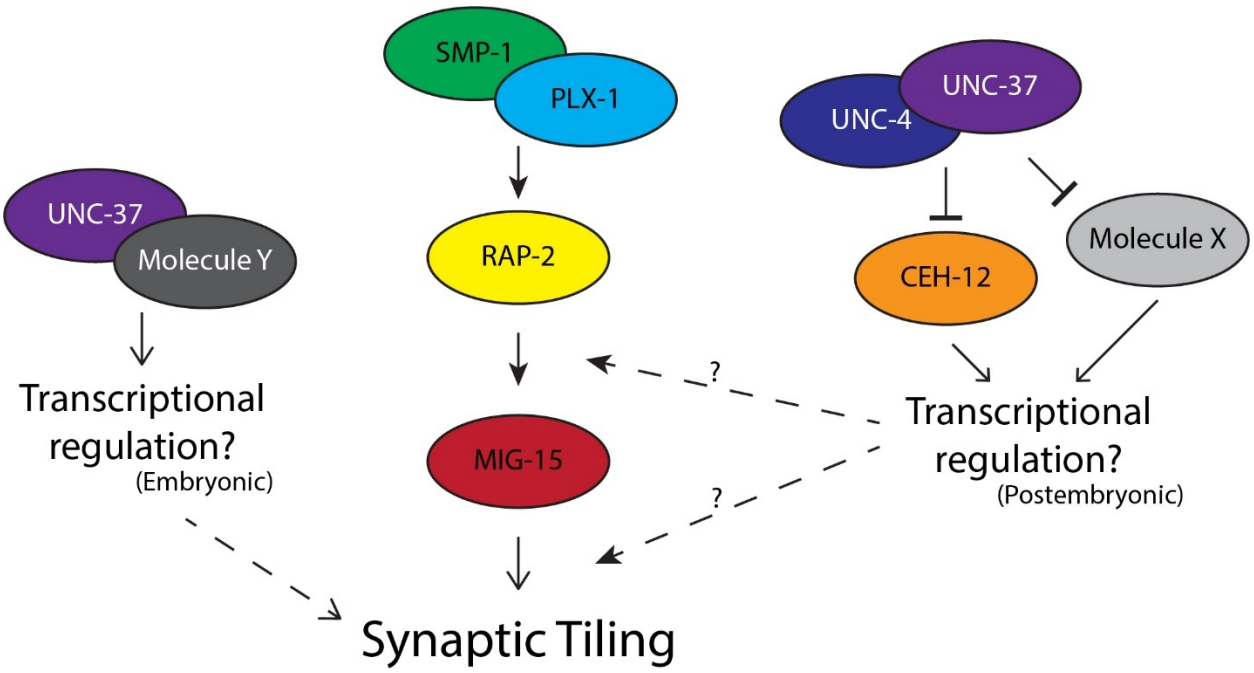

Figure 15. Schematic of the interactions between UNC-4 and UNC-37 and the PLX-1 signaling cascade in synaptic tiling.

smp-1/plx-1 signaling cascade is required for the synaptic tiling of the DA8 and DA9 neurons. *unc-4* and *unc-37* function together to regulate synaptic tiling. *unc-4* functions post-embryonically in regulating synaptic tiling, whereas *unc-37* is required in both embryonic and post-embryonic stages in DA neurons. *unc-4* and *unc-37* function in the same genetic pathway as *plx-1* signaling cascade. *unc-4* inhibits the expression of *ceh-12* in DA neurons. *ceh-12* likely functions downstream of *unc-4* and *unc-37* along with redundant genes to regulate synaptic tiling. Filled arrows represent known genetic pathway. Hammerheads represent negative regulation. Line arrows represent functional pathway. Dotted filled arrows represent genetic interactions that have fully been identified yet. Dotted line arrows represent unknown interactions.

4. Discussion

In this study, we provide evidence that the cell fate determinant of DA and VA neurons, *unc*-4 and its co-repressor *unc-37*, have novel roles in the postmitotic DA neurons to fine tune the patterning of presynaptic innervation. Previous studies in both vertebrates and invertebrate system have demonstrated that sustained expression of neuronal cell fate determinants in the postmitotic differentiated neurons is required to maintain effector gene expression for the functionality of neurons. Furthermore, some neuronal transcriptional regulators are required for proper neuronal connectivity (Howell et al., 2015; Pereira et al., 2015; Kratsios et al., 2015; Seroka and Doe, 2019; Lacin et al., 2020). We found that the synaptic tiling of DA8 and DA9 cholinergic motor neurons is completely abolished in *unc-4* and *unc-37* mutant animals. Interestingly, we found that *unc-4* and *unc-37* function together in synaptic tiling but are required at temporal distinct timepoints (post-embryonically vs embryonic and post-embryonic).

The transcriptional co-repressor Groucho/TLE family proteins are abundant and important regulators of development in invertebrates and vertebrates (reviewed in Buscarlet and Stifani, 2007). The role of Groucho/TLE proteins has been described in most detail in neurogenesis (Gasperowicz and Otto, 2005). In *C. elegans*, *unc-37* is involved in several developmental processes including asymmetric cell division of the seam cells, apoptosis of the male-specific CEM neurons in hermaphrodites, and development of ASE neurons (Zhang and Emmons, 2002; Peden et al., 2007; Chang et al., 2003; Flowers et al., 2010). Furthermore, the interaction of *unc-37* with *unc-4* in VA motor neuron identity and circuit wiring has been well established (Pflugrad et al., 1997; Winnier et al., 1999; Von Stetina et al., 2006). Here, we find that *unc-37* has a role in regulating the synaptic pattern formation of DA8 and DA9 neurons in an *unc-4*-dependent manner post-embryonically, and an *unc-4*-independent embryonic unknown

pathway. Generally, UNC-37 interacts with EH1 domain-containing homeobox proteins such as UNC-4, COG-1, or MAB-9 (Winnier et al., 1999; Chang et al., 2003; Jafari et al., 2011) and can also dimerize with Groucho-related proteins via a Q-rich domain (Flowers et al., 2010) and physically interact with histone deacetylases such as in the *hda-1/pop-1* complex (Calvo et al., 2001). It is likely that UNC-37 functions in DA neurons by forming a complex with unidentified transcription factors during the embryonic development, in addition to the *unc-4* pathway to regulate tiled innervation in the postmitotic DA neurons. Further biochemical studies to pull-down binding partners would elucidate the molecular mechanism of the *unc-4*-independent *unc-37* parallel pathway.

While we have shown that the loss of *unc-4* and *unc-37* causes ectopic expression of *ceh-12* in DA neurons, and the ectopic overexpression of *ceh-12* in DA neurons is sufficient to cause synaptic tiling defects, suggesting *ceh-12* functions downstream of *unc-4/unc-37* in synaptic tiling. However, the inability of loss of *ceh-12* to suppress synaptic tiling of *unc-4* and *unc-37* mutants suggest that there are possible redundant downstream effectors of *unc-4* and *unc-37.* A similar finding has been observed with the role of *ceh-12* in VA neurons to control synaptic choice (Von Stetina et al., 2006). While transgenic expression of *ceh-12* in VA neurons was sufficient to induce *unc-4*-like movement defects in wildtype animals, the loss of *ceh-12* in *unc-4* and *unc-37* mutant backgrounds did not fully rescue the locomotion defect or the ectopic gap junctions formed between VA and AVA interneurons. Previous study has identified that *egl-20/Wnt* and its receptors *mom-5/fz* and *mig-1/fz* functions antagonistically with *unc-4* and *unc-37* to regulate the expression of *ceh-12* in the posterior VA neurons in *C. elegans* where expression of *egl-20* is localized (Schneider et al., 2012). The loss of *egl-20, mom-5,* or *mig-1* causes decreased ectopic expression of *ceh-12* in the posterior VA neurons in *unc-4* mutant

backgrounds. Therefore, it is possible that *egl-20* also functions antagonistically with *unc-4* to regulate downstream effectors including *ceh-12* in tiled synaptic innervation.

There has been a growing effort to elucidate the postmitotic roles of neuronal cell fate determinants in many organisms including *C. elegans*. Many of the postmitotic roles of these neuronal cell fate determinants shows the maintenance of neuronal identity (Kratsios et al., 2011; Deneris and Hobert, 2014; Alqadah et al., 2015; Hobert, 2016). While Kratsios et al., 2015 has shown that *unc-3*, the terminal selector for cholinergic motor neurons in *C. elegans*, can regulate synaptogenesis of the SAB cholinergic motor neuron through *madd-4* gene expression, and the Miller Lab has provided examples of neuronal cell fate determinants disrupting neuronal circuitry (Miller et al., 1992; Pflugrad, et al., 1997; Winnier et al., 1999; Von Stetina et al., 2007; Feinberg et al., 2008), the postmitotic role of neuronal cell fate determinants on synaptic wiring has not been shown. Here we have provided evidence that neuronal cell fate determinants *unc-4* and *unc-37* have significant roles in postmitotic neurons to regulate synapse pattern formation in *C. elegans.*

An important question arising from our study is whether neuronal cell fate transcription factors of other motor neuron classes may also control the synaptic tiled innervation of their respective neuronal class. For example, in VB and DB motor neuron classes, which utilize VAB-7 as a transcriptional repressor (Esmaeilli et al., 2002), would we see synaptic tiling defects in *vab-7* mutants, similar to *unc-4* mutant animals? Unfortunately, the loss of *vab-7* causes reversed axonal polarity, in which B-class motor neurons which normally extend their axons posteriorly now extend anteriorly, thereby making such results difficult to interpret (Esmaeilli et al., 2002). However, the emergence of the auxin-inducible degradation (AID) system would allow researchers to study the post-embryonic roles of genes such as *vab-7* which would otherwise

cause developmental defects. By inserting an AID-degron tag in the endogenous of locus of *vab-7* and expressing TIR1 in B-type cholinergic motor neurons, spatial and temporal degradation of VAB-7 is possible by controlling the Auxin treatment.

Previous electron microscopy reconstruction has revealed the tiled synaptic innervation of *C. elegans* motor neurons, including cholinergic motor neurons defined by *unc-3* (White et al., 1986). We have previously proposed that DA8 and DA9 neurons utilize the Semaphorin-Plexin signaling pathway with an unidentified molecule on the DA8 neuron to specify the tiling border of the DA8 and DA9 synaptic domains. However, it is unclear if each class of neurons utilises their own specific signaling pathway and/or cell surface proteins to dictate the tiling borders of individual neuron classes. It is possible that terminal selectors and their transcriptional repressors that define motor neuron classes act as a co-regulatory strategy to differentially express cell surface proteins or cell surface protein isoforms required for the tiled innervation. However, as previously mentioned, loss of terminal selectors hinders our ability to visualize specific neuronal classes due to the use of class-specific promoters which are often downstream effectors of the terminal selector in question. However, the reversibility of the AID system allows the degradation of these transcription factors such as UNC-3, and upon transferring the mutant animals onto control plates, we can rescue the degradation of UNC-3 and visualise the synaptic defects. Utilizing the AID-system would help bypass many of the limitations of studying the role of terminal selectors in synapse formation and synaptic patterning in other neurons.

5. References

1 Allan, D. W., Park, D., St Pierre, S. E., Taghert, P. H. & Thor, S. Regulators acting in combinatorial codes also act independently in single differentiating neurons. *Neuron* **45**, 689-700, doi:10.1016/j.neuron.2005.01.026 (2005).

2 Allan, D. W. & Thor, S. Transcriptional selectors, masters, and combinatorial codes: regulatory principles of neural subtype specification. *Wiley Interdiscip Rev Dev Biol* **4**, 505-528, doi:10.1002/wdev.191 (2015).

3 Alqadah, A. *et al.* Postmitotic diversification of olfactory neuron types is mediated by differential activities of the HMG-box transcription factor SOX-2. *EMBO J* **34**, 2574-2589, doi:10.15252/embj.201592188 (2015).

4 Altun-Gultekin, Z. *et al.* A regulatory cascade of three homeobox genes, *ceh-10, ttx-3* and *ceh-23*, controls cell fate specification of a defined interneuron class in C. elegans. *Development* **128**, 1951-1969 (2001).

5 Armenti, S. T., Lohmer, L. L., Sherwood, D. R. & Nance, J. Repurposing an endogenous degradation system for rapid and targeted depletion of *C. elegans* proteins. *Development* **141**, 4640-4647, doi:10.1242/dev.115048 (2014).

6 Bahrampour, S., Gunnar, E., Jonsson, C., Ekman, H. & Thor, S. Neural Lineage Progression Controlled by a Temporal Proliferation Program. *Dev Cell* **43**, 332-348 e334, doi:10.1016/j.devcel.2017.10.004 (2017).

7 Baumgardt, M., Karlsson, D., Terriente, J., Diaz-Benjumea, F. J. & Thor, S. Neuronal subtype specification within a lineage by opposing temporal feed-forward loops. *Cell* **139**, 969-982, doi:10.1016/j.cell.2009.10.032 (2009).

8 Baumgardt, M., Miguel-Aliaga, I., Karlsson, D., Ekman, H. & Thor, S. Specification of neuronal identities by feedforward combinatorial coding. *PLoS Biol* **5**, e37, doi:10.1371/journal.pbio.0050037 (2007).

9 Bayraktar, O. A. & Doe, C. Q. Combinatorial temporal patterning in progenitors expands neural diversity. *Nature* **498**, 449-455, doi:10.1038/nature12266 (2013).

10 Benito-Sipos, J. *et al.* A genetic cascade involving *klumpfuss, nab* and *castor* specifies the abdominal leucokinergic neurons in the *Drosophila* CNS. *Development* **137**, 3327-3336, doi:10.1242/dev.052233 (2010).

11 Brenner, S. The genetics of Caenorhabditis elegans. *Genetics* **77**, 71-94 (1974).

12 Brose, K. *et al.* Slit proteins bind Robo receptors and have an evolutionarily conserved role in repulsive axon guidance. *Cell* **96**, 795-806 (1999).

13 Burglin, T. R. Homeodomain subtypes and functional diversity. *Subcell Biochem* **52**, 95-122, doi:10.1007/978-90-481-9069-0_5 (2011).

14 Buscarlet, M. & Stifani, S. The 'Marx' of Groucho on development and disease. *Trends Cell Biol* **17**, 353-361, doi:10.1016/j.tcb.2007.07.002 (2007).

15 Calvo, D. *et al.* A POP-1 repressor complex restricts inappropriate cell type-specific gene transcription during *Caenorhabditis elegans* embryogenesis. *EMBO J* **20**, 7197-7208, doi:10.1093/emboj/20.24.7197 (2001).

16 Carney, T. D., Struck, A. J. & Doe, C. Q. *midlife crisis* encodes a conserved zinc-finger protein required to maintain neuronal differentiation in *Drosophila*. *Development* **140**, 4155-4164, doi:10.1242/dev.093781 (2013).

17 Chalfie, M. *et al.* The neural circuit for touch sensitivity in *Caenorhabditis elegans*. *J Neurosci* **5**, 956-964 (1985).

18 Chang, S., Johnston, R. J., Jr. & Hobert, O. A transcriptional regulatory cascade that controls left/right asymmetry in chemosensory neurons of *C. elegans*. *Genes & development* **17**, 2123-2137, doi:10.1101/gad.1117903 (2003).

19 Chen, J., Rattner, A. & Nathans, J. The rod photoreceptor-specific nuclear receptor Nr2e3 represses transcription of multiple cone-specific genes. *J Neurosci* **25**, 118-129, doi:10.1523/JNEUROSCI.3571-04.2005 (2005).
20 Chen, S. *et al.* Crx, a novel Otx-like paired-homeodomain protein, binds to and transactivates photoreceptor cell-specific genes. *Neuron* **19**, 1017-1030, doi:10.1016/s0896-6273(00)80394-3 (1997).
21 Chen, X. *et al.* Rap2 and TNIK control Plexin-dependent tiled synaptic innervation in *C. elegans*. *eLife* **7**, doi:10.7554/eLife.38801 (2018).
22 Cheng, A., Wang, S., Cai, J., Rao, M. S. & Mattson, M. P. Nitric oxide acts in a positive feedback loop with BDNF to regulate neural progenitor cell proliferation and differentiation in the mammalian brain. *Developmental biology* **258**, 319-333, doi:10.1016/s0012-1606(03)00120-9 (2003).
23 Cho, H. H. *et al. Isl1* directly controls a cholinergic neuronal identity in the developing forebrain and spinal cord by forming cell type-specific complexes. *PLoS Genet* **10**, e1004280, doi:10.1371/journal.pgen.1004280 (2014).
24 Christoffels, V. M., Keijser, A. G., Houweling, A. C., Clout, D. E. & Moorman, A. F. Patterning the embryonic heart: identification of five mouse Iroquois homeobox genes in the developing heart. *Developmental biology* **224**, 263-274, doi:10.1006/dbio.2000.9801 (2000).
25 Cinar, H., Keles, S. & Jin, Y. Expression profiling of GABAergic motor neurons in *Caenorhabditis elegans*. *Curr Biol* **15**, 340-346, doi:10.1016/j.cub.2005.02.025 (2005).
26 Dasen, J. S. *et al.* Temporal regulation of a paired-like homeodomain repressor/TLE corepressor complex and a related activator is required for pituitary organogenesis. *Genes & development* **15**, 3193-3207, doi:10.1101/gad.932601 (2001).
27 Deneris, E. S. & Hobert, O. Maintenance of postmitotic neuronal cell identity. *Nature neuroscience* **17**, 899-907, doi:10.1038/nn.3731 (2014).
28 Dharmasiri, N., Dharmasiri, S. & Estelle, M. The F-box protein TIR1 is an auxin receptor. *Nature* **435**, 441-445, doi:10.1038/nature03543 (2005).
29 Ding, Y. Q. *et al. Lmx1b* is essential for the development of serotonergic neurons. *Nature neuroscience* **6**, 933-938, doi:10.1038/nn1104 (2003).
30 Doe, C. Q. Temporal Patterning in the *Drosophila* CNS. *Annu Rev Cell Dev Biol* **33**, 219-240, doi:10.1146/annurev-cellbio-111315-125210 (2017).
31 Doitsidou, M. *et al.* A combinatorial regulatory signature controls terminal differentiation of the dopaminergic nervous system in *C. elegans*. *Genes & development* **27**, 1391-1405, doi:10.1101/gad.217224.113 (2013).
32 Eastman, C., Horvitz, H. R. & Jin, Y. Coordinated transcriptional regulation of the *unc-25* glutamic acid decarboxylase and the *unc-47* GABA vesicular transporter by the *Caenorhabditis elegans* UNC-30 homeodomain protein. *J Neurosci* **19**, 6225-6234 (1999).
33 Elshatory, Y., Deng, M., Xie, X. & Gan, L. Expression of the LIM-homeodomain protein Isl1 in the developing and mature mouse retina. *The Journal of comparative neurology* **503**, 182-197, doi:10.1002/cne.21390 (2007).
34 Erclik, T. *et al.* Integration of temporal and spatial patterning generates neural diversity. *Nature* **541**, 365-370, doi:10.1038/nature20794 (2017).
35 Ericson, J., Thor, S., Edlund, T., Jessell, T. M. & Yamada, T. Early stages of motor neuron differentiation revealed by expression of homeobox gene *Islet-1*. *Science* **256**, 1555-1560, doi:10.1126/science.1350865 (1992).
36 Esmaeili, B., Ross, J. M., Neades, C., Miller, D. M., 3rd & Ahringer, J. The *C. elegans* even-skipped homologue, *vab-7*, specifies DB motoneurone identity and axon trajectory. *Development* **129**, 853-862 (2002).
37 Etchberger, J. F. *et al.* The molecular signature and cis-regulatory architecture of a *C. elegans* gustatory neuron. *Genes & development* **21**, 1653-1674, doi:10.1101/gad.1560107 (2007).

38 Flames, N. & Hobert, O. Gene regulatory logic of dopamine neuron differentiation. *Nature* **458**, 885-889, doi:10.1038/nature07929 (2009).
39 Flowers, E. B. *et al.* The Groucho ortholog UNC-37 interacts with the short Groucho-like protein LSY-22 to control developmental decisions in *C. elegans. Development* **137**, 1799-1805, doi:10.1242/dev.046219 (2010).
40 Fox, R. M. *et al.* A gene expression fingerprint of *C. elegans* embryonic motor neurons. *BMC Genomics* **6**, 42, doi:10.1186/1471-2164-6-42 (2005).
41 Friedland, A. E. *et al.* Heritable genome editing in *C. elegans* via a CRISPR-Cas9 system. *Nat Methods* **10**, 741-743, doi:10.1038/nmeth.2532 (2013).
42 Frokjaer-Jensen, C. *et al.* Single-copy insertion of transgenes in *Caenorhabditis elegans*. *Nat Genet* **40**, 1375-1383, doi:10.1038/ng.248 (2008).
43 Frokjaer-Jensen, C. *et al.* Random and targeted transgene insertion in *Caenorhabditis elegans* using a modified Mos1 transposon. *Nat Methods* **11**, 529-534, doi:10.1038/nmeth.2889 (2014).
44 Furukawa, T., Morrow, E. M. & Cepko, C. L. *Crx*, a novel otx-like homeobox gene, shows photoreceptor-specific expression and regulates photoreceptor differentiation. *Cell* **91**, 531-541, doi:10.1016/s0092-8674(00)80439-0 (1997).
45 Gasperowicz, M. & Otto, F. Mammalian Groucho homologs: redundancy or specificity? *J Cell Biochem* **95**, 670-687, doi:10.1002/jcb.20476 (2005).
46 Gehring, W. J., Affolter, M. & Burglin, T. Homeodomain proteins. *Annu Rev Biochem* **63**, 487-526, doi:10.1146/annurev.bi.63.070194.002415 (1994).
47 Hasegawa, E., Kaido, M., Takayama, R. & Sato, M. Brain-specific-homeobox is required for the specification of neuronal types in the *Drosophila* optic lobe. *Developmental biology* **377**, 90-99, doi:10.1016/j.ydbio.2013.02.012 (2013).
48 Hedgecock, E. M., Culotti, J. G. & Hall, D. H. The *unc-5, unc-6*, and *unc-40* genes guide circumferential migrations of pioneer axons and mesodermal cells on the epidermis in *C. elegans*. *Neuron* **4**, 61-85 (1990).
49 Hendi, A., Kurashina, M. & Mizumoto, K. Intrinsic and extrinsic mechanisms of synapse formation and specificity in *C. elegans*. *Cell Mol Life Sci* **76**, 2719-2738, doi:10.1007/s00018-019-03109-1 (2019).
50 Hendricks, T., Francis, N., Fyodorov, D. & Deneris, E. S. The ETS domain factor Pet-1 is an early and precise marker of central serotonin neurons and interacts with a conserved element in serotonergic genes. *J Neurosci* **19**, 10348-10356 (1999).
51 Hirono, K., Kohwi, M., Clark, M. Q., Heckscher, E. S. & Doe, C. Q. The Hunchback temporal transcription factor establishes, but is not required to maintain, early-born neuronal identity. *Neural Dev* **12**, 1, doi:10.1186/s13064-017-0078-1 (2017).
52 Hobert, O. Terminal Selectors of Neuronal Identity. *Curr Top Dev Biol* **116**, 455-475, doi:10.1016/bs.ctdb.2015.12.007 (2016).
53 Hobert, O. A map of terminal regulators of neuronal identity in *Caenorhabditis elegans*. *Wiley Interdiscip Rev Dev Biol* **5**, 474-498, doi:10.1002/wdev.233 (2016).
54 Hobert, O. & Kratsios, P. Neuronal identity control by terminal selectors in worms, flies, and chordates. *Current opinion in neurobiology* **56**, 97-105, doi:10.1016/j.conb.2018.12.006 (2019).
55 Holguera, I. & Desplan, C. Neuronal specification in space and time. *Science* **362**, 176-180, doi:10.1126/science.aas9435 (2018).
56 Howell, K., White, J. G. & Hobert, O. Spatiotemporal control of a novel synaptic organizer molecule. *Nature* **523**, 83-87, doi:10.1038/nature14545 (2015).
57 Ishii, N., Wadsworth, W. G., Stern, B. D., Culotti, J. G. & Hedgecock, E. M. UNC-6, a laminin-related protein, guides cell and pioneer axon migrations in *C. elegans*. *Neuron* **9**, 873-881 (1992).
58 Jafari, G., Appleford, P. J., Seago, J., Pocock, R. & Woollard, A. The UNC-4 homeobox protein represses *mab-9* expression in DA motor neurons in *Caenorhabditis elegans*. *Mech Dev* **128**, 49-58, doi:10.1016/j.mod.2010.09.005 (2011).

59 Jin, Y., Hoskins, R. & Horvitz, H. R. Control of type-D GABAergic neuron differentiation by *C. elegans* UNC-30 homeodomain protein. *Nature* **372**, 780-783, doi:10.1038/372780a0 (1994).
60 Jorgensen, E. M. & Nonet, M. L. Neuromuscular junctions in the nematode *C. elegans*. *Seminars in Developmental Biology* **6**, 207-220, doi:https://doi.org/10.1016/S1044-5781(06)80030-7 (1995).
61 Kadkhodaei, B. *et al.* Nurr1 is required for maintenance of maturing and adult midbrain dopamine neurons. *J Neurosci* **29**, 15923-15932, doi:10.1523/JNEUROSCI.3910-09.2009 (2009).
62 Kepinski, S. & Leyser, O. The Arabidopsis F-box protein TIR1 is an auxin receptor. *Nature* **435**, 446-451, doi:10.1038/nature03542 (2005).
63 Kerk, S. Y., Kratsios, P., Hart, M., Mourao, R. & Hobert, O. Diversification of *C. elegans* Motor Neuron Identity via Selective Effector Gene Repression. *Neuron* **93**, 80-98, doi:10.1016/j.neuron.2016.11.036 (2017).
64 Kidd, T., Bland, K. S. & Goodman, C. S. Slit is the midline repellent for the robo receptor in *Drosophila*. *Cell* **96**, 785-794 (1999).
65 Klassen, M. P. & Shen, K. Wnt signaling positions neuromuscular connectivity by inhibiting synapse formation in *C. elegans*. *Cell* **130**, 704-716, doi:10.1016/j.cell.2007.06.046 (2007).
66 Konstantinides, N. *et al.* Phenotypic Convergence: Distinct Transcription Factors Regulate Common Terminal Features. *Cell* **174**, 622-635 e613, doi:10.1016/j.cell.2018.05.021 (2018).
67 Konstantinides, N., Rossi, A. M. & Desplan, C. Common temporal identity factors regulate neuronal diversity in fly ventral nerve cord and mouse retina. *Neuron* **85**, 447-449, doi:10.1016/j.neuron.2015.01.016 (2015).
68 Kratsios, P. *et al.* An intersectional gene regulatory strategy defines subclass diversity of *C. elegans* motor neurons. *eLife* **6**, doi:10.7554/eLife.25751 (2017).
69 Kratsios, P. *et al.* Transcriptional coordination of synaptogenesis and neurotransmitter signaling. *Curr Biol* **25**, 1282-1295, doi:10.1016/j.cub.2015.03.028 (2015).
70 Kratsios, P., Stolfi, A., Levine, M. & Hobert, O. Coordinated regulation of cholinergic motor neuron traits through a conserved terminal selector gene. *Nature neuroscience* **15**, 205-214, doi:10.1038/nn.2989 (2011).
71 Lacin, H., Williamson, W. R., Card, G. M., Skeath, J. B. & Truman, J. W. Unc-4 acts to promote neuronal identity and development of the take-off circuit in the *Drosophila* CNS. *eLife* **9**, doi:10.7554/eLife.55007 (2020).
72 Leitges, M., Neidhardt, L., Haenig, B., Herrmann, B. G. & Kispert, A. The paired homeobox gene *Uncx4.1* specifies pedicles, transverse processes and proximal ribs of the vertebral column. *Development* **127**, 2259-2267 (2000).
73 Lewis, E. B. A gene complex controlling segmentation in *Drosophila*. *Nature* **276**, 565-570, doi:10.1038/276565a0 (1978).
74 Li, W., Kang, L., Piggott, B. J., Feng, Z. & Xu, X. Z. The neural circuits and sensory channels mediating harsh touch sensation in *Caenorhabditis elegans*. *Nat Commun* **2**, 315, doi:10.1038/ncomms1308 (2011).
75 Li, X., Chen, Z. & Desplan, C. Temporal patterning of neural progenitors in *Drosophila*. *Curr Top Dev Biol* **105**, 69-96, doi:10.1016/B978-0-12-396968-2.00003-8 (2013).
76 Li, X. *et al.* Temporal patterning of *Drosophila* medulla neuroblasts controls neural fates. *Nature* **498**, 456-462, doi:10.1038/nature12319 (2013).
77 Liang, X. *et al. Isl1* is required for multiple aspects of motor neuron development. *Mol Cell Neurosci* **47**, 215-222, doi:10.1016/j.mcn.2011.04.007 (2011).
78 Mansouri, A., Voss, A. K., Thomas, T., Yokota, Y. & Gruss, P. *Uncx4.1* is required for the formation of the pedicles and proximal ribs and acts upstream of *Pax9*. *Development* **127**, 2251-2258 (2000).
79 Mansouri, A. *et al.* Paired-related murine homeobox gene expressed in the developing sclerotome, kidney, and nervous system. *Dev Dyn* **210**, 53-65, doi:10.1002/(SICI)1097-0177(199709)210:1<53::AID-AJA6>3.0.CO;2-0 (1997).

80 Mattar, P., Ericson, J., Blackshaw, S. & Cayouette, M. A conserved regulatory logic controls temporal identity in mouse neural progenitors. *Neuron* **85**, 497-504, doi:10.1016/j.neuron.2014.12.052 (2015).
81 McGinnis, W. & Krumlauf, R. Homeobox genes and axial patterning. *Cell* **68**, 283-302, doi:10.1016/0092-8674(92)90471-n (1992).
82 McGinnis, W., Levine, M. S., Hafen, E., Kuroiwa, A. & Gehring, W. J. A conserved DNA sequence in homoeotic genes of the *Drosophila Antennapedia* and *bithorax* complexes. *Nature* **308**, 428-433, doi:10.1038/308428a0 (1984).
83 McKim, K. S., Starr, T. & Rose, A. M. Genetic and molecular analysis of the *dpy-14* region in *Caenorhabditis elegans*. *Mol Gen Genet* **233**, 241-251, doi:10.1007/BF00587585 (1992).
84 Mears, A. J. *et al. Nrl* is required for rod photoreceptor development. *Nat Genet* **29**, 447-452, doi:10.1038/ng774 (2001).
85 Miller, D. M., 3rd & Niemeyer, C. J. Expression of the *unc-4* homeoprotein in *Caenorhabditis elegans* motor neurons specifies presynaptic input. *Development* **121**, 2877-2886 (1995).
86 Miller, D. M., 3rd, Niemeyer, C. J. & Chitkara, P. Dominant *unc-37* mutations suppress the movement defect of a homeodomain mutation in unc-4, a neural specificity gene in *Caenorhabditis elegans*. *Genetics* **135**, 741-753 (1993).
87 Miller, D. M. *et al. C. elegans* unc-4 gene encodes a homeodomain protein that determines the pattern of synaptic input to specific motor neurons. *Nature* **355**, 841-845, doi:10.1038/355841a0 (1992).
88 Miller, R. R. & Okkema, P. G. The *Caenorhabditis elegans* T-box factor MLS-1 requires Groucho co-repressor interaction for uterine muscle specification. *PLoS Genet* **7**, e1002210, doi:10.1371/journal.pgen.1002210 (2011).
89 Mizumoto, K. & Shen, K. Interaxonal interaction defines tiled presynaptic innervation in *C. elegans*. *Neuron* **77**, 655-666, doi:10.1016/j.neuron.2012.12.031 (2013).
90 Monedero Cobeta, I., Salmani, B. Y. & Thor, S. Anterior-Posterior Gradient in Neural Stem and Daughter Cell Proliferation Governed by Spatial and Temporal Hox Control. *Curr Biol* **27**, 1161-1172, doi:10.1016/j.cub.2017.03.023 (2017).
91 Muhr, J., Andersson, E., Persson, M., Jessell, T. M. & Ericson, J. Groucho-mediated transcriptional repression establishes progenitor cell pattern and neuronal fate in the ventral neural tube. *Cell* **104**, 861-873, doi:10.1016/s0092-8674(01)00283-5 (2001).
92 Nishimura, K., Fukagawa, T., Takisawa, H., Kakimoto, T. & Kanemaki, M. An auxin-based degron system for the rapid depletion of proteins in nonplant cells. *Nat Methods* **6**, 917-922, doi:10.1038/nmeth.1401 (2009).
93 Nusslein-Volhard, C. & Wieschaus, E. Mutations affecting segment number and polarity in *Drosophila*. *Nature* **287**, 795-801, doi:10.1038/287795a0 (1980).
94 Obinata, H., Sugimoto, A. & Niwa, S. Streptothricin acetyl transferase 2 (*Sat2*): A dominant selection marker for *Caenorhabditis elegans* genome editing. *PLoS One* **13**, e0197128, doi:10.1371/journal.pone.0197128 (2018).
95 Peden, E., Kimberly, E., Gengyo-Ando, K., Mitani, S. & Xue, D. Control of sex-specific apoptosis in *C. elegans* by the BarH homeodomain protein CEH-30 and the transcriptional repressor UNC-37/Groucho. *Genes & development* **21**, 3195-3207, doi:10.1101/gad.1607807 (2007).
96 Pereira, L. *et al.* A cellular and regulatory map of the cholinergic nervous system of *C. elegans*. *eLife* **4**, doi:10.7554/eLife.12432 (2015).
97 Perry, M., Konstantinides, N., Pinto-Teixeira, F. & Desplan, C. Generation and Evolution of Neural Cell Types and Circuits: Insights from the *Drosophila* Visual System. *Annu Rev Genet* **51**, 501-527, doi:10.1146/annurev-genet-120215-035312 (2017).
98 Pfaff, S. L., Mendelsohn, M., Stewart, C. L., Edlund, T. & Jessell, T. M. Requirement for LIM homeobox gene *Isl1* in motor neuron generation reveals a motor neuron-dependent step in interneuron differentiation. *Cell* **84**, 309-320, doi:10.1016/s0092-8674(00)80985-x (1996).

99 Pflugrad, A., Meir, J. Y., Barnes, T. M. & Miller, D. M., 3rd. The Groucho-like transcription factor UNC-37 functions with the neural specificity gene *unc-4* to govern motor neuron identity in *C. elegans*. *Development* **124**, 1699-1709 (1997).
100 Regulski, M. *et al.* Homeo box genes of the *Antennapedia* and *bithorax* complexes of *Drosophila*. *Cell* **43**, 71-80, doi:10.1016/0092-8674(85)90013-3 (1985).
101 Rehemtulla, A. *et al.* The basic motif-leucine zipper transcription factor Nrl can positively regulate rhodopsin gene expression. *Proc Natl Acad Sci U S A* **93**, 191-195, doi:10.1073/pnas.93.1.191 (1996).
102 Sammeta, N., Hardin, D. L. & McClintock, T. S. Uncx regulates proliferation of neural progenitor cells and neuronal survival in the olfactory epithelium. *Mol Cell Neurosci* **45**, 398-407, doi:10.1016/j.mcn.2010.07.013 (2010).
103 Schneider, J. *et al.* UNC-4 antagonizes Wnt signaling to regulate synaptic choice in the *C. elegans* motor circuit. *Development* **139**, 2234-2245, doi:10.1242/dev.075184 (2012).
104 Scott, M. P., Tamkun, J. W. & Hartzell, G. W., 3rd. The structure and function of the homeodomain. *Biochim Biophys Acta* **989**, 25-48, doi:10.1016/0304-419x(89)90033-4 (1989).
105 Serafini, T. *et al.* The netrins define a family of axon outgrowth-promoting proteins homologous to *C. elegans* UNC-6. *Cell* **78**, 409-424 (1994).
106 Seroka, A. Q. & Doe, C. Q. The Hunchback temporal transcription factor determines motor neuron axon and dendrite targeting in *Drosophila*. *Development* **146**, doi:10.1242/dev.175570 (2019).
107 Serrano-Saiz, E., Leyva-Diaz, E., De La Cruz, E. & Hobert, O. BRN3-type POU Homeobox Genes Maintain the Identity of Mature Postmitotic Neurons in Nematodes and Mice. *Curr Biol* **28**, 2813-2823 e2812, doi:10.1016/j.cub.2018.06.045 (2018).
108 Shan, G., Kim, K., Li, C. & Walthall, W. W. Convergent genetic programs regulate similarities and differences between related motor neuron classes in *Caenorhabditis elegans*. *Developmental biology* **280**, 494-503, doi:10.1016/j.ydbio.2005.01.032 (2005).
109 Sullivan, L. F., Warren, T. L. & Doe, C. Q. Temporal identity establishes columnar neuron morphology, connectivity, and function in a *Drosophila* navigation circuit. *eLife* **8**, doi:10.7554/eLife.43482 (2019).
110 Sulston, J. E. Neuronal cell lineages in the nematode *Caenorhabditis elegans*. *Cold Spring Harb Symp Quant Biol* **48 Pt 2**, 443-452, doi:10.1101/sqb.1983.048.01.049 (1983).
111 Sulston, J. E. & Horvitz, H. R. Post-embryonic cell lineages of the nematode, *Caenorhabditis elegans*. *Developmental biology* **56**, 110-156, doi:10.1016/0012-1606(77)90158-0 (1977).
112 Sulston, J. E., Schierenberg, E., White, J. G. & Thomson, J. N. The embryonic cell lineage of the nematode *Caenorhabditis elegans*. *Developmental biology* **100**, 64-119, doi:10.1016/0012-1606(83)90201-4 (1983).
113 Suzuki, T., Kaido, M., Takayama, R. & Sato, M. A temporal mechanism that produces neuronal diversity in the *Drosophila* visual center. *Developmental biology* **380**, 12-24, doi:10.1016/j.ydbio.2013.05.002 (2013).
114 Thompson-Peer, K. L., Bai, J., Hu, Z. & Kaplan, J. M. HBL-1 patterns synaptic remodeling in *C. elegans*. *Neuron* **73**, 453-465, doi:10.1016/j.neuron.2011.11.025 (2012).
115 Thor, S. & Thomas, J. B. The *Drosophila* islet gene governs axon pathfinding and neurotransmitter identity. *Neuron* **18**, 397-409, doi:10.1016/s0896-6273(00)81241-6 (1997).
116 Tsuchida, T. *et al.* Topographic organization of embryonic motor neurons defined by expression of LIM homeobox genes. *Cell* **79**, 957-970, doi:10.1016/0092-8674(94)90027-2 (1994).
117 Uchida, O., Nakano, H., Koga, M. & Ohshima, Y. The *C. elegans che-1* gene encodes a zinc finger transcription factor required for specification of the ASE chemosensory neurons. *Development* **130**, 1215-1224, doi:10.1242/dev.00341 (2003).
118 Vollmer, J. Y. & Clerc, R. G. Homeobox genes in the developing mouse brain. *J Neurochem* **71**, 1-19, doi:10.1046/j.1471-4159.1998.71010001.x (1998).

119 Von Stetina, S. E. *et al.* UNC-4 represses CEH-12/HB9 to specify synaptic inputs to VA motor neurons in *C. elegans. Genes & development* **21**, 332-346, doi:10.1101/gad.1502107 (2007).
120 Wang, H. F. & Liu, F. C. Developmental restriction of the LIM homeodomain transcription factor Islet-1 expression to cholinergic neurons in the rat striatum. *Neuroscience* **103**, 999-1016, doi:10.1016/s0306-4522(00)00590-x (2001).
121 Watanabe, S. *et al.* Ultrafast endocytosis at *Caenorhabditis elegans* neuromuscular junctions. *eLife* **2**, e00723, doi:10.7554/eLife.00723 (2013).
122 Wenick, A. S. & Hobert, O. Genomic cis-regulatory architecture and trans-acting regulators of a single interneuron-specific gene battery in *C. elegans*. *Dev Cell* **6**, 757-770, doi:10.1016/j.devcel.2004.05.004 (2004).
123 White, J. G., Southgate, E. & Thomson, J. N. Mutations in the *Caenorhabditis elegans* unc-4 gene alter the synaptic input to ventral cord motor neurons. *Nature* **355**, 838-841, doi:10.1038/355838a0 (1992).
124 White, J. G., Southgate, E., Thomson, J. N. & Brenner, S. The structure of the nervous system of the nematode *Caenorhabditis elegans*. *Philos Trans R Soc Lond B Biol Sci* **314**, 1-340, doi:10.1098/rstb.1986.0056 (1986).
125 Winnier, A. R. *et al.* UNC-4/UNC-37-dependent repression of motor neuron-specific genes controls synaptic choice in *Caenorhabditis elegans*. *Genes & development* **13**, 2774-2786, doi:10.1101/gad.13.21.2774 (1999).
126 Wyler, S. C. *et al.* Pet-1 Switches Transcriptional Targets Postnatally to Regulate Maturation of Serotonin Neuron Excitability. *J Neurosci* **36**, 1758-1774, doi:10.1523/JNEUROSCI.3798-15.2016 (2016).
127 Xia, D., Zhang, Y., Huang, X., Sun, Y. & Zhang, H. The C. elegans CBFbeta homolog, BRO-1, regulates the proliferation, differentiation and specification of the stem cell-like seam cell lineages. *Developmental biology* **309**, 259-272, doi:10.1016/j.ydbio.2007.07.020 (2007).
128 Zhang, F. *et al.* The LIM and POU homeobox genes *ttx-3* and *unc-86* act as terminal selectors in distinct cholinergic and serotonergic neuron types. *Development* **141**, 422-435, doi:10.1242/dev.099721 (2014).
129 Zhang, L., Ward, J. D., Cheng, Z. & Dernburg, A. F. The auxin-inducible degradation (AID) system enables versatile conditional protein depletion in *C. elegans*. *Development* **142**, 4374-4384, doi:10.1242/dev.129635 (2015).
130 Zhou, H. M. & Walthall, W. W. UNC-55, an orphan nuclear hormone receptor, orchestrates synaptic specificity among two classes of motor neurons in *Caenorhabditis elegans*. *J Neurosci* **18**, 10438-10444 (1998).